5-2004

Synthesis and Initial Characterization of a Calcium-Deficient Hydroxyapatite-Bacterial Cellulose Composite

Stacy Hutchens
University of Tennessee - Knoxville

To the Graduate Council:

I am submitting herewith a thesis written by Stacy Hutchens entitled "Synthesis and Initial Characterization of a Calcium-Deficient Hydroxyapatite-Bacterial Cellulose Composite." I have examined the final electronic copy of this thesis for form and content and recommend that it be accepted in partial fulfillment of the requirements for the degree of Master of Science, with a major in Engineering Science.

Richard Jendrucko, Major Professor

We have read this thesis and recommend its acceptance:

Roberto Benson, Hugh O'Neil

Accepted for the Council:
Carolyn R. Hodges

Vice Provost and Dean of the Graduate School

(Original signatures are on file with official student records.)

To the Graduate Council:

I am submitting herewith a thesis written by Stacy Hutchens entitled "Synthesis and Initial Characterization of a Calcium-Deficient Hydroxyapatite-Bacterial Cellulose Composite." I have examined the final electronic copy of this thesis for form and content and recommend that it be accepted in partial fulfillment of the requirements for the degree of Master of Science, with a major in Engineering Science.

Richard Jendrucko

Dr. Richard Jendrucko, Major Professor

We have read this thesis
and recommend its acceptance:

Roberto Benson

Dr. Roberto Benson

Hugh O'Neill

Dr. Hugh O'Neill

Accepted for the Council:

Anne Mayhew

Vice Chancellor and Dean of Graduate Studies

(Original signatures are on file with official student records)

Synthesis and Initial Characterization of a Calcium-Deficient Hydroxyapatite-Bacterial Cellulose Composite

A Thesis Presented for the Master of Science Degree

The University of Tennessee, Knoxville

Stacy Hutchens
May 2004

Dedication

This thesis is dedicated to my parents: Larry and Monina Hutchens. Their encouragement and inspiration fuel the fulfillment of my goals. Thanks also to Paul, for being a great brother and friend.

In addition, this thesis is dedicated to my loving boyfriend, Emil, whose support and understanding enabled this achievement.

Acknowledgments

I am very grateful to the National Science Foundation whose generous grant supports my work.

I wish to thank everyone who made my masters education possible. I am indebted to Dr. Jonathan Woodward for inviting me to Oak Ridge National Laboratory and introducing me to such a rewarding project. Much gratitude to Dr. Barbara Evans who has been a constant source of knowledge and support. I am thankful to Dr. Hugh O'Neill for all his help and putting up with all my questions. Thanks to my advisor, Dr. Richard Jendrucko, whose coordination and facilitation enabled my thesis to happen. Thank you Dr. Roberto Benson for your insight in the biomaterial characterization and testing processes. I would also like to thank Dr. Steve Kennel's group, namely Linda Foote, at Oak Ridge National Laboratory for letting me use their facilities for the mammalian cell culturing. I am obliged to Dr. David Beach letting me use his x-ray diffraction machine, and also to Dr. Madhavi Martin for performing the Laser Induced Breakdown Spectroscopy. Thanks also to Dr. Claudia Rawn for instructing me on the x-ray diffraction machine at the High Temperature Materials Laboratory* at Oak Ridge National Laboratory.

*Research sponsored by the Assistant Secretary for Energy Efficiency and Renewable Energy, Office of FreedomCAR and Vehicle Technologies, as part of the High Temperature Materials Laboratory User Program, Oak Ridge National Laboratory, managed by UT-Battelle, LLC, for the U.S. Department of Energy under contract number DE-AC05-00OR22725.

Abstract

Bacterial cellulose is a biopolymer currently being investigated for use in a variety of biomedical applications. It has high purity, extensive hydrophilicity, and superior mechanical properties. A novel composite was developed consisting of bioceramic particles precipitated in bacterial cellulose. Alizarin Red S staining was first used to indicate the presence of calcium. Laser-Induced Breakdown Analysis confirmed the presence of calcium and phosphorus in the cellulose matrix. X-ray diffraction was finally used to identify the precipitated minerals. Incubating the cellulose in aqueous calcium chloride followed by incubation in sodium phosphate dibasic produced calcium-deficient hydroxyapatite. Incubation in calcium chloride and sodium carbonate solutions produced calcium carbonate. Bacterial cellulose was incubated in simulated body fluid to ascertain how it would react in an artificial physiological environment. In-vitro testing with osteoblasts was also conducted to assess its biocompatibility. By performing cell counts and an alkaline phosphatase assay, it was proven that the osteoblasts preferentially attached to the hydroxyapatite bacterial cellulose versus native bacterial cellulose. The bacterial cellulose-hydroxyapatite composite is synthesized by incubation in aqueous salt solutions at physiological pH and ambient temperature. This contrasts other hydroxyapatite synthesis methods that use harsh chemicals (e.g. orthophosphoric acid) at extreme temperature or pressure conditions (hydrothermal reactions at 275ºC / 12000 psi). Combining hydroxyapatite into bacterial cellulose may generate a composite with favorable mechanical and chemical properties that are appropriate for various medical applications.

Table of Contents

List of Tables

List of Figures

Chapter 1

Introduction

This thesis describes the synthesis and initial characterization of a novel composite biomaterial. A technique has been developed that produces bioceramic particles in a bacterial cellulose matrix (1). Simulating bone, this method is a simple process of incubating the cellulose in aqueous salt solutions containing calcium and phosphorus ions. X-ray diffraction was used to identify the mineral deposit from one of the techniques as calcium-deficient hydroxyapatite, while another technique produced calcium carbonate. Cellulose also conducts apatite when placed in simulated body fluid. Phosphorylated cellulose mineralized as well. Preliminary in-vitro testing indicates that this material is non-toxic and may be compatible with bone. Previous investigations utilizing bacterial cellulose and calcium-deficient hydroxyapatite in medical devices uphold the hypothesis that this novel composite could be a successful biomaterial.

1.1 Calcium Phosphate Bioceramics

1.1.1 Ceramics in Medicine

Ceramics have been used for over a hundred years to replace hard tissues in the body (2). Bone consists of inorganic mineral crystals arranged in an organic collagen matrix. Consequently, scientists have looked to ceramics that are naturally present in the bone when constructing ceramic bone implants. Many mineral phases occur in bone, but the most predominant constituent is a calcium phosphate mineral resembling hydroxyapatite (HAP) ($Ca_{10}(PO_4)_6(OH)_2$). Other minor minerals such as brushites ($CaHPO_4$) and carbonates ($CaCO_3$) are also present in lower concentrations (3).

Calcium phosphate minerals are biocompatible ceramics that have been proven effective in replacing bone. Inert ceramics like alumina tend to be encapsulated by fibrous tissue when implanted in the body, preventing the formation of a chemically bonded interface. Calcium phosphate bioceramics, on the other hand, have bioactive properties that permit a direct bond to form between the implant and the tissue (2). This phenomenon is called osteoconduction (4).

1.1.2 Influence of Calcium Phosphate Composition to Performance

Calcium phosphate ceramics perform differently when implanted in the body based on chemical composition, morphology, crystallinity, crystal size, and crystal shape will affect the attachment and function of the ceramic (3,5,6).

Calcium phosphate minerals can take on several chemical compositions depending on the conditions of synthesis. The performance of the minerals after implantation varies based on the ratio of calcium to phosphorus (3) (Table 1.1).

In a paper by de Groot, the effectiveness of various calcium phosphates in in-vivo models was discussed (3). Sintered or powdered calcium phosphates with a Ca:P ratio less than one tend to quickly be absorbed into the body without therapeutic effect. Hydrated and glass calcium phosphates with a Ca:P ratio less than one had slight healing effects. Calcium phosphates with Ca:P ratios between one and two form a tight bond with bone when implanted. They also produce an apatitic structure when placed in serum. Overall, it was seen that as the Ca:P ratio

Table 1.1: Types of Calcium Phosphate

Name	Stoichiometry	Calcium to Phosphorus Ratio
Tetracalcium Phosphate	$Ca_4P_2O_9$	0.5
Monocalcium Phosphate	$Ca(H_2PO_4)_2$	0.5
Monocalcium Phosphate Monohydrate	$Ca(H_2PO_4)_2{\cdot}H_2O$	0.5
Tricalcium Phosphate / Amorphous Calcium Phosphate	$Ca_2(PO_4)_3$	0.667
Monetite / Calcium Monophosphate	$CaHPO_4$	1
Brushite	$CaHPO_4$	1
Dicalcium Phosphate Dihydrate	$CaHPO_4 \cdot 2H_2O$	1
Calcium Pyrophosphate	$Ca_2P_2O_7$	1
Octacalcium Phosphate	$Ca_8H_2(PO_4)_6$	1.333
Calcium Phosphate Tribasic / Whitlocke / Oxydapatite	$Ca_3(PO_4)_2$	1.5
Hydroxyapatite / Hydroxylapatite / Durapatite	$Ca_{10}(PO_4)_6(OH)_2$	1.667
Calcium Tetraphosphate	$Ca_4P_2O_4$	2

(3)

increases, the rate of degradability of the calcium phosphate decreases (3).

The presence of different phases in the calcium phosphate affects the mechanical properties and biocompatibility of the overall mineral. For example, Royer et al. found that hydroxyapatite containing tricalcium phosphate had higher flexural strength than hydroxyapatite alone (5). Many other papers have commented that a "biphasic" hydroxyapatite containing tricalcium phosphate promoted osteoconduction more thoroughly and faster than hydroxyapatite alone (7,8).

The properties of calcium phosphates also depend on their physical form. Dense calcium phosphates form a bond with bone only at the interface and degrade very slowly. Porous calcium phosphates enable bone growth within the material pores and are degradable through extracellular dissolution and intracellular digestion. Rate of dissolution can also depend on the presence of trace elements (3).

Size and shape of calcium phosphate particles also impact biocompatibility. In studies by Laquerriere et al., it was seen that needle shaped particles elicited a greater inflammatory response than round particles. It was also shown that smaller particles (1-30μm) induced more of an inflammatory response than larger particles (170-300μm) (6).

1.1.3 Synthesis of Hydroxyapatite

Hydroxyapatite for biomaterial application is typically synthesized in one of four ways: precipitation, hydrothermal techniques, hydrolysis, or via sol gels. Most frequently used is the precipitation technique. This procedure usually entails the combination of either calcium hydroxide and orthophosphoric acid or calcium nitrate and diammonium hydrogen phosphate. The former combination requires a slow reaction process at a pH > 9 at temperatures varying between 25 and 90°C. The latter combination is faster, but rigorous washing of the precipitated HAP is required at the end of the reaction to remove the nitrates and ammonium hydroxide (9).

Hydrothermal reactions are the second most common HAP synthesis technique. This method entails mixing calcium carbonate with diammonium hydrogen phosphate at very high

temperatures and pressures, such as 275°C and 12,000 psi. The resultant hydroxyapatite is substituted with carbonate and not stoichiometric (9).

A new synthesis method has recently been developed that produces hydroxyapatite in a process more similar to the physiological formation of apatites. This involves the use of simulated body fluid (SBF); a salt solution whose ion concentration nearly equals that of human blood plasma. Kokubo et al. first discovered the formation of poorly crystallized apatite on glass-ceramics when placed in simulated body fluid (10).

Certain functional groups nucleate apatite when in contact with simulated body fluid. This mechanism entails the formation of atomic clusters from the supersaturated aqueous media onto the functional groups. These functional groups include carboxyl groups, phosphate groups, and hydroxyl groups. It is believed the atomic clusters form a calcium phosphate precursor of the form $Ca_3(PO_4)_2$. The $Ca_3(PO_4)_2$ units eventually transition to hydroxyapatite (11).

Kokubo et al. have used this technique to precipitate apatite on metals and polymers (11). Tas combined the technique of Kokubo with the conventional HAP precipitation technique (utilizing calcium nitrate and ammonium phosphate dissolved in SBF) to produce HAP powders (12).

Apatite formed in simulated body fluid has been termed "bone-like apatite" because its composition and structure are similar to that of bone mineral. It has been demonstrated that bone-like apatite formed from simulated body fluid promotes bone integration. Osteoblasts have been observed to preferentially proliferate on the bone-like apatite and differentiate to form natural bone (11).

Employing this "biomimetic" technique with other materials may produce additional ceramic composite materials that induce bone formation and osteoblast attachment.

1.1.4 Calcium-Deficient Hydroxyapatite Versus Stoichiometric Hydroxyapatite

Stoichiometric hydroxyapatite (sHAP) is represented by the compound $Ca_{10}(PO_4)_6(OH)_2$. Fully calcium-deficient hydroxyapatite (CdHAP) takes on the form $Ca_9(HPO_4)(PO_4)_5(OH)$. Physiological HAP is almost always calcium deficient compared to stoichiometric hydroxyapatite

due to contact with a constant flow of trace ions. Physiological apatite can take on the form $Ca_{10-x}(HPO_4)_x(PO_4)_{6-x}(OH)_{2-x}$ with $0< x \leq 1$ (13).

Calcium deficient hydroxyapatite dissolves faster in aqueous environments than stoichiometric hydroxyapatite. Mavropoulos et al. synthesized several CdHAP samples with decreasing Ca:P ratios and incubated them in water for 7 days at 37C. Dissolution consists of calcium and phosphate detachment from the apatite surface. The concentration of calcium and phosphorus in the solution was analyzed using inductively-coupled plasma optical emission spectrometry. CdHAP samples with lower Ca:P ratios (1.5-1.55) detached much more calcium and phosphorus ions than those with higher ratios (1.6-1.65) indicating a higher dissolution rate (Figure 1.1) (14). Stoichiometric hydroxyapatite, with a solubility product constant of 115.5 at 25°C, dissolves much slower than CdHAP (15).

Due to slower dissolution, stoichiometric hydroxyapatite is clinically used as a long-term implant. It is often used in maxillofacial reconstruction for bone augmentation. Calcium-deficient

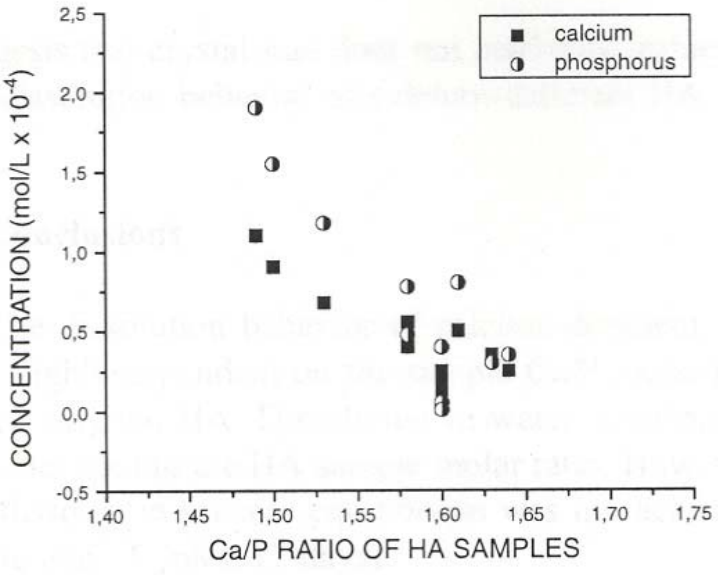

Figure 1.1: Solution Composition of HAP Samples after Dissolution Test (14)

hydroxyapatite dissolves faster than sHAP. It is more appropriate as a temporary implant material that will eventually be replaced by bone (16). These implants are used for temporary bone space fillers or in the treatment of long bone fractures (2).

Studies have shown that CdHAP bonds with bone more quickly than SHAP. In a study by Lin et al., it was shown that CdHAP immediately became covered in precipitated apatite when incubated in simulated body fluid (17). sHAP also precipitated apatite, but at a much slower rate (17). This thick layer of biomimetic apatite may contribute to a better bond with bone. It has been seen that apatites (such as CdHAP) that are able to undergo surface modifications once implanted exhibit excellent tissue response. The stability and resistance to dissolution prevents sHAP from enabling surface modification (18).

An in-vivo study with CdHAP was conducted in 2003 by Bourgeois et al. (19). CdHAP induced rapid bone colonization with nearly complete degradation after two weeks. Stoichiometric hydroxyapatite generated much less bone formation. CdHAP also has a large specific surface area which facilitates the loading of therapeutic agents which may further increase bone cell colonization (19). In orthopedic applications, rapid incorporation of an implant may eliminate the need for a second surgery.

Ducheyne et al. compiled a variety of events that were reported to occur at a bioactive ceramic-tissue interface (18). These events are illustrated in Figure 1.2 on the following page and are listed as follows: 1) dissolution of the ceramic, 2) precipitation from solution onto the ceramic, 3) ion exchange and structural rearrangement at the ceramic-tissue interface, 4) interdiffusion from the surface boundary layer into the ceramic, 5) solution-mediated effects on cellular activity, 6) deposition of either the a) mineral phase b) or organic phase without integration into the ceramic surface, 7) deposition with integration into the ceramic, 8) chemotaxis to the ceramic surface, 9) cell attachment and proliferation, 10) cell differentiation, and 11) extracellular matrix formation (18).

The limited bioactivity of sHAP can be attributed to its slow dissolution rate. The precursor phases of bone formation are dependent on the ability of a ceramic to dissolve,

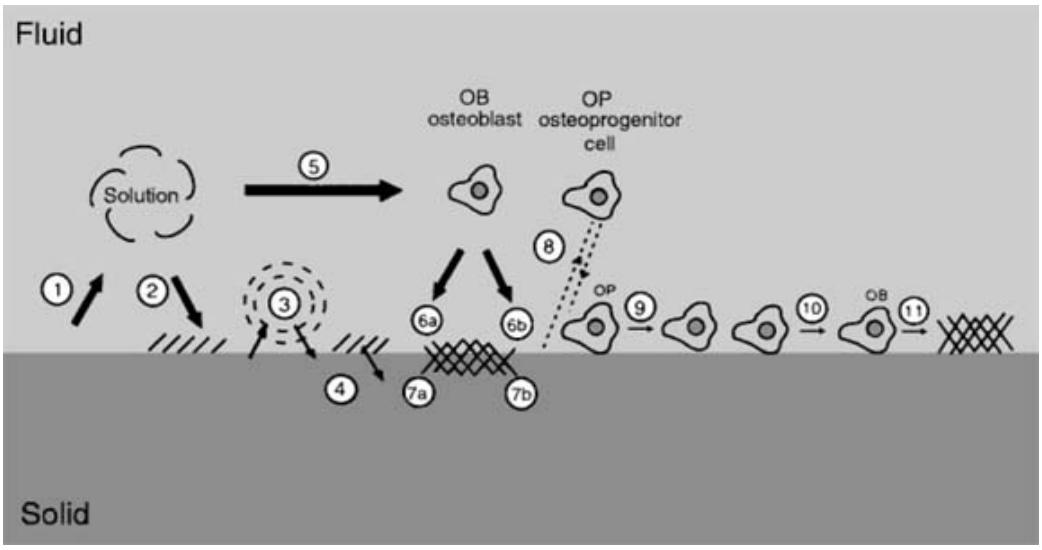

Figure 1.2: Schematic Drawing of Events Occurring at the Bioactive Tissue-Ceramic Interface

(18)

precipitate ions from surrounding solution, and permission of ion exchange at the ceramic-tissue interface. This permits cellular adhesion and matrix deposition. Though sHAP eventually does dissolve resulting in a bioactive ceramic-tissue interface, it takes much longer than apatites with faster dissolution rates. The solubility of calcium-deficient apatite enables a bioactive ceramic-tissue interface to form faster, as was observed in the previously mentioned in-vivo testing (19).

1.2 Ceramic-Polymer Composites

A composite material consists of two or more distinct substances. Composite materials are developed so that the favorable properties of each of the components may form a single structurally complementary material. Composite materials contain functional properties that are not present in the individual components (20).

Ceramic-polymer composites consist of a discontinuous phase of ceramic particles embedded within a continuous polymer matrix. Polymers have low fracture strength and become reinforced by the strength and hardness of the ceramic particles. Ceramics are rigid and

fracture easily, but the polymer matrix enables the stresses to be transferred to the ceramic component in such a way that the particles can bear the load (20).

1.2.1 Advantages of Ceramic-Polymer Composites in Medicine

In the past, ceramics have been typically chosen as substitutes for bone due to their strength, resistance to fatigue, and bioactivity. However, the mechanical properties of physiological bone vary from those of ceramic materials significantly. Most notably is the higher elastic modulus of ceramics, which can be up to 10-20 times that of bone (21). This high level of stiffness leads to brittle and weak behavior when loaded under tension or shear (22). Because of the brittle nature and low fracture toughness of ceramics, their applications are limited to implant coatings or low-loaded implants.

When an implant whose stiffness greatly contrasts that of the surrounding bone, a problematic phenomenon called “stress-shielding” or “stress-protection” occurs. Stress-shielding negatively affects desired bone remodeling by increasing overall bone porosity and inducing atrophy. Implanting a material with stiffness similar to bone enables normal tissue remodeling (21).

As mentioned earlier, bone consists of hydroxyapatite-like crystals embedded in a matrix of collagen fibrils. In other words, bone is a ceramic-polymer composite. A rational conclusion is that a ceramic-polymer composite should be developed to substitute bone. Natural collagen is costly to harvest and short in supply. It is thus necessary to seek other materials to replace the function of a collagen carrier for apatite.

Polymers are an ideal choice for this function. They can be made in a variety of compositions and forms to feature diverse mechanical and chemical properties. Fiber reinforced polymers, like collagen, have a very low modulus of elasticity and high tensile strength (21).

Combining polymers with ceramics can produce a material whose overall mechanical properties closely resemble bone. By containing bioceramic particles, the composite can feature bone-bonding properties. Countless combinations of polymers and ceramics could be manufactured and modified to feature specific mechanical and chemical properties. Resorbable

polymers could be utilized to enable the ceramic particles to come in close contact with the bone during tissue growth. Polymer-ceramic composites could also be specially designed to mimic the anisotropic properties present in bone (21).

1.2.2 Examples of Ceramic-Polymer Composites

There have been numerous composites developed in recent years for medical devices that feature calcium phosphate ceramics in polymer carriers (Table 1.2).

There is a seemingly endless assortment of synthetic polymers being developed and improved upon each day. Synthetic polymers are fabricated to feature a variety of properties at a low price (23). Polyethylene is a common polymeric biomaterial found in hip and knee implants. Bonfield et al. produced a composite by depositing bioactive hydroxyapatite particles in polyethylene which had a Young's modulus comparable to bone (1-8 GPa). The interaction mechanism between the HAP particles and the polyethylene was not reported. However, the composite featured low surface area of the HAP particles which limited the bioactivity of the ceramic (21). Polyetheretherketone (PEEK) has found extensive applications in industry due

Table 1.2: Polymer Carriers used for Calcium Phosphate Ceramics in Previous Work

Category of Polymer	Type of Polymer
Synthetic Polymers	Polyethylene (24)
	Polyetheretherketone (PEEK) (25)
	Polymethylmethacrylate (PMMA) (26)
	Polyethylmethacyrlate (PEMA) (26)
	Poly(hexamethylene adipamide) (27)
	Polysulfone (28)
	Silicone (29)
	Polylactic Acid (PLA) (30)
	Poly(lactide-co-glycolide) Acid (PLGA) (30)
Natural Polymers	Gelatin (31)
	Chitin (32)
	Chitosan (33)
	Chitosan-Gelatin Network (34)
	Alginate (35)
	Plant Cellulose (36)
	Starch Copolymer (37)
	Gellan (32)

to its favorable mechanical and chemical properties. When combined with HAP particles, the overall Young's Modulus and tensile strength were comparable with that of cortical bone (25). However, during cyclic loading, fracture damage was observed due to the debonding of the HAP particles in the PEEK matrix indicating poor interfacial interaction (25). Much more research and development must be conducted with synthetic polymer-ceramic composites to attain an ideal bone substitute.

Though synthetic polymers have a variety of favorable properties, drawbacks do exist. Processing synthetic polymers may utilize non-renewable resources and produce environmentally unfriendly waste products. For example, in the synthesis of polyethylene, ethylene monomer is polymerized using highly active metallic catalysts. As polymerization proceeds, the reactive mixture is scrubbed with dilute aqueous caustic solutions that become high volume pollutants in the wastewater stream (38). The polymers may also retain unreacted monomers or chemicals utilized during fabrication. In medical applications, these residues could induce inflammatory reactions once implanted.

Natural polymers may be an effective alternative. Biopolymers are an essential component of living organisms, functioning both as chemical activators and for structural support. Fabricated natural polymers mimic the structure of proteins and polysaccharides found in the extracellular matrices of tissues. They are derived from renewable sources and are biodegradable (39).

However, there are problems with the use of natural polymer-ceramic composites as well. Though Oliveira et al. were able to grow a thick layer of apatite on a starch composite, starch-based polymers change the composition and the pH of the surrounding environment during degradation (37). Chang et al. deposited hydroxyapatite nanocrystals onto gelatin fibrils on the nanoscale range. However, the inability of gelatin to form long-range fibrils hinders the development of an effective network structure (31).

1.2.3 Polysaccharide Biopolymers as Biomaterials

One class of natural polymers that shows promise as a biomaterial is polysaccharides. Polysaccharides are carbohydrate polymers found in plant and animal tissues. In humans, glycosaminoglycans are polysaccharides that covalently bond with proteins to form the structural components of tissue. Hyaluronic acid is a polysaccharide found in tissue, the synovial fluid of joints, and the vitreous humor of the eyes. Plant polysaccharides like starch provide food storage, while plant cellulose provides structural support (40).

Many polysaccharide materials, such as chitosan, dextran, alginate, and agarose; are being developed for medical applications (41). One of the most important properties of polysaccharides is their ability to form a network structure, or a hydrogel. Because most of the human body is water, and almost all chemical reactions in the body occur in water; it is favorable to have a hydrophilic material for implantation (41).

In the family of biomaterials, cellulose is an established archetype. This polysaccharide has been utilized in the production of dialysis membranes since the 1940s (42). It has also since been employed as a drug-coating material and as a blood coagulant (42).

1.3 Bacterial Cellulose

1.3.1 Cellulose: Plant Vs. Bacterial

Cellulose is the most abundant natural polymer in the world. Being the primary component of plant cell walls, an estimated 10^{10}-10^{11} tons of cellulose are naturally produced each year (40). Though plants produce most cellulose, certain bacterial species possess the ability to secrete pure cellulose (43). Though identical in chemical composition, the structure of plant and bacterial cellulose varies, as do their mechanical properties (Table 1.3, following page). The main function of plant cellulose is to provide structure for the vegetable fibers. It is linked with other polymers such as hemicellulose and lignin to form a rigid matrix. Extracting cellulose from these polymers requires harsh chemical processes, such as treatment with sulfuric acid. This often causes the cellulose to lose strength.

Cellulose produced by microorganisms is in the form of microfibrils that are much smaller

Table 1.3: Differences in Structural/Mechanical Properties of Plant Cellulose (Cotton Linters) and Bacterial Cellulose (from *Acetobacter xylinus*)

	Bacterial Cellulose	Plant Cellulose
Fibril Width Size (42,43)	70-80 nm	0.01-0.03 mm
Degree of Polymerization (44,45)	1,000-4,000	8,000-10,000
Young's Modulus (46)	15-30 GPa	5.5-12.6 GPa
Water Retention Value (47,48)	1000%	50%
Purification Process	Incubate in water	Bleach and scour

than those in plant cellulose (Figure 1.3, following page). It is synthesized in a pure state, unlinked with any other polymer. Unlike fibrous plant cellulose, bacterial cellulose (BC) is an extensively-hydrated hydrogel. Though the precise function of the bacterial cellulose is not confirmed. Some biologists believe the bacteria construct the cellulose "cage" to protect themselves from harmful agents such as ultraviolet light or heavy metal ions (48).

Bacterial cellulose, like plant cellulose, is mostly made up of the crystalline form Cellulose I. Cellulose I is made of chains arranged uniaxially, giving a crystalline structure. Cellulose I can take the form Cellulose I_α which has a triclinic unit cell, or Cellulose I_β which has a monoclinic unit cell. Plant cellulose tends to have less Cellulose I_α than bacterial cellulose. It has been reported that the predominant Cellulose I_α in bacterial cellulose makes it more crystalline (43).

Bacterial cellulose is commercialized as a food product, a speaker component, and recently as a medical device. It comprises a Filipino food product called Nata de Coco that has been produced for the past 70 years. Only recently, Sony® began manufacturing speakers and headphones with acoustic diaphragms made of dried bacterial cellulose. A Brazilian company called Allvet Química Industrial Ltd. distributes an FDA approved bacterial cellulose wound dressing called Biofill®. A new American company called Xylos Corporation (Langhorne, Pennsylvania) also produces a bacterial cellulose wound dressing product called XCELL™.

1.3.2 Chemical Structure of Bacterial Cellulose

The chemical structure of bacterial cellulose is typical of a polysaccharide. Polysaccharides consist of monosaccharide monomer units called sugars. A sugar residue is in

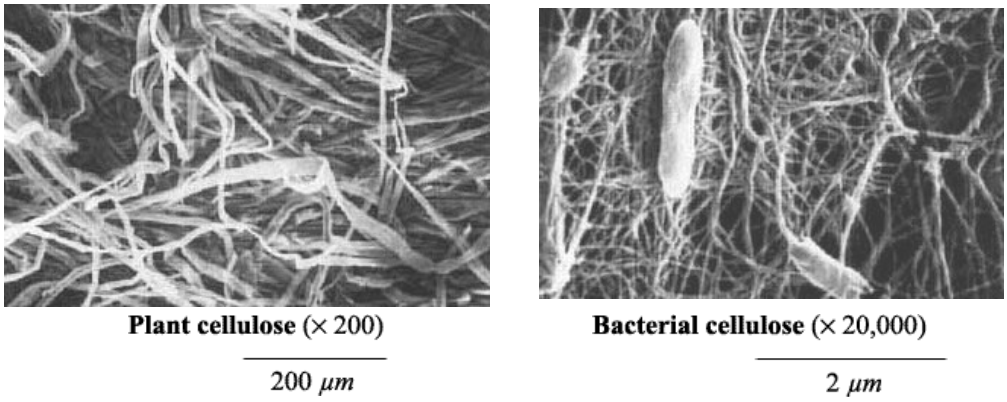

Figure 1.3: Comparison of Plant Cellulose Fibrils and Bacterial Cellulose Fibrils

Images taken from http://www.res.titech.ac.jp/~junkan/english/cellulose/

the form of a six-membered pyranose ring that is linked to other residues by glycosidic bonds. The monosaccharides of cellulose are β-(1,4) glucan sugars. Position 1 on one pyranose ring is linked to position 4 on the adjacent ring (Figure 1.4.A, following page) (40).

The β-(1,4)-glucan chains are laterally bonded to other via hydrogen bonds between the hydroxyl functional groups (Figure 1.4.B, following page). Linkages are formed within the saccharide chain (intrafibrillar hydrogen bonding) and between saccharide chains (interfibrillar hydrogen bonding).

1.3.3 Bacterial Assembly of Cellulose

Bacterial species that produce cellulose, such as *Sarcina, Agrobacterium, Rhizobium,* and *Gluconoacetobacter;* are aerobic organisms that are gram-negative and rod-shaped. In nature, these bacteria are found in rotting fruits and vegetables. Adrian Brown first identified bacterial cellulose in 1886 when he found a "slippery skin" on the surface of vinegar ferment and characterized it as cellulose (49).

In the laboratory, cellulose-producing bacteria can be cultivated in a liquid media containing sources of carbon and nitrogen (50). Within a few days, the bacteria will form a

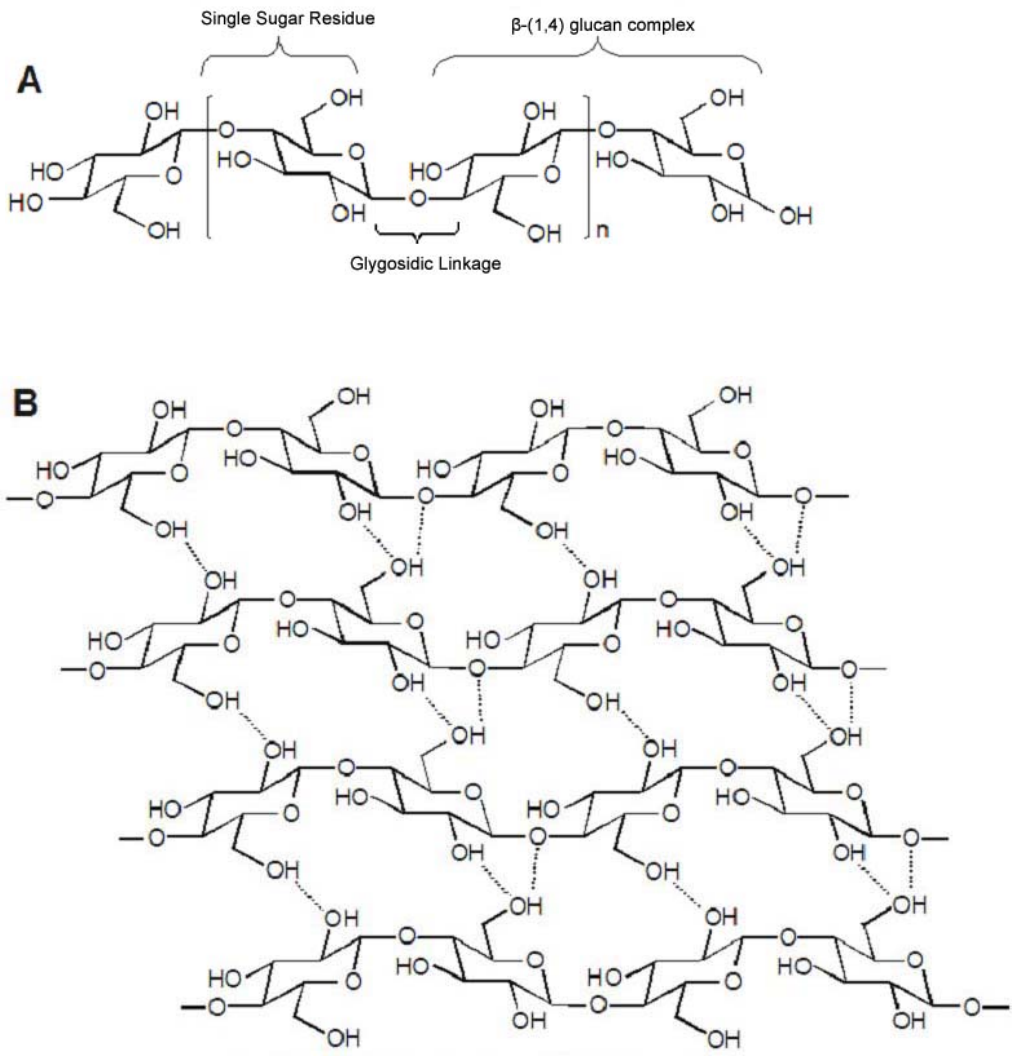

Figure 1.4: Chemical Structure of Cellulose

A: Cellulose chain, n = 2,000 to 10,000
B: Cellulose network, dotted lines indicate intermolecular hydrogen bonds

Image created on ChemDraw®

gelatinous membrane on the air-liquid interface termed a “pellicle.” The thickness of the pellicle increases over time, but growth tends to slow down after about 10 days (51).

Along the longitudinal axis of the bacteria cell are a series of pores where the cellulose chains are extruded (Figure 1.5, following page). The bacterium produces approximately 10-100 cellulose chains which aggregate into microfibrils with a width of 1.5nm. These microfibrils in turn extracellularly bundle to form ribbons that are 3-4 nm thick and 70-80 nm wide. The ribbons twist and overlap to form parallel crystal lattice planes which stack on top of each other to form the thickness of the pellicle (Figure 1.6, following page) (43).

The microfibrils are bonded together with hydrogen bonds to form the escalating ribbon, plane layer, and pellicle structures. Because the size of the microfibrils is so fine, there is a great deal of contact area between them. This causes the density of inter- and intrafibrillar hydrogen bonds to be very high. The profuse secondary bonding gives the cellulose its hydrogel structure. It also gives the cellulose great mechanical strength and water retention (1000%) (48,52). Water consists of 99.8% of total volume of bacterial cellulose (53).

Once dried down, the array of fibers and intrafibrillar hydrogen bonds collapse. The interfibrillar hydrogen bonds remain, producing a film of very high tensile strength. Yamanaka reported that the Young’s Modulus of a sheet of dried bacterial cellulose was around 15 GPa, but could be high as 30 GPa with extensive purification (54). The cellulose “paper” that results from dehydration is a very strong material that can be used as acoustic diaphragms in stereo speakers (46). Once dried down, the intrafibrillar hydrogen bonds cannot form again. For this reason, the dried cellulose remains as a film and cannot re-swell into the three-dimensional pellicle network. At this time, the elastic modulus of hydrated cellulose could not be found in the literature.

1.3.4 Modification of Bacterial Cellulose

The chemical and physical structure of cellulose enables it to be modified by various methods. These modifications can be used to improve its mechanical, chemical, and biological properties. This is very important when designing a biomaterial which can be used in different applications.

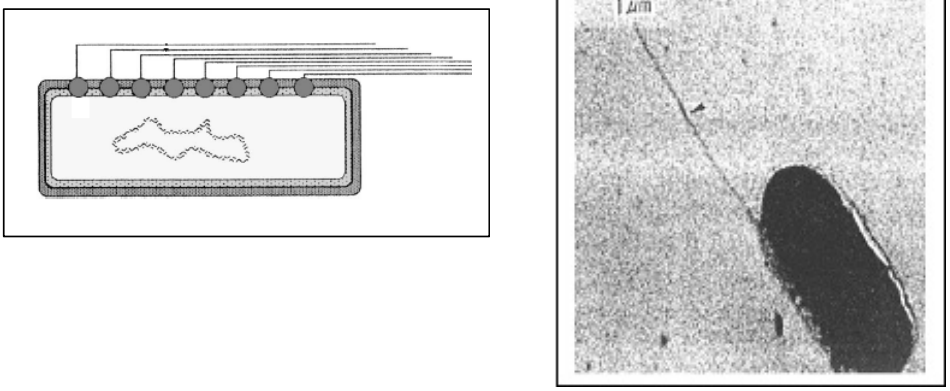

Figure 1.5: Diagram of Cellulose Extrusion by Bacteria

Left: Each bacteria cell produces 10-100 cellulose chains from separate pores along their longitudinal axis. The chains aggregate into microfibrils which bundle into ribbons
Right: Extrusion of the cellulose ribbon from bacteria

(48)

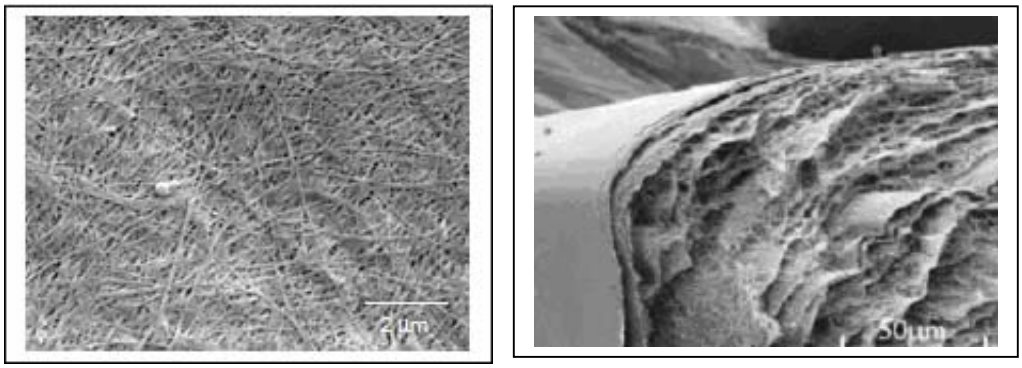

Figure 1.6: Formation of Three Dimensional Network in Bacterial Cellulose

Left: Cellulose ribbons twist and overlap to form a parallel lattice crystal plane
Right: The planes stack on top of each other to form the thickness of the pellicle

Micrographs taken at Oak Ridge National Laboratory

1.3.4.a Culture Modifications

During culture, the cellulose is "self-assembled" by the bacteria into a well-organized fibril network. The structure of the network determines the chemical and physical properties of the cellulose. However, it is possible to alter the synthesis conditions of the cultured bacteria to change the properties of the formed cellulose. The porosity of the pellicles can be modified by using a different carbon source (fructose, mannitol, corn syrup) or a using synthetic growth media that consists of only inorganic components (55).

The cellulose can be directly synthesized into specific shapes during culture using gas-permeable membranes. The bacteria are aerobic, and the active cellulose-producing bacteria exist at the surface (dormant bacteria are also present within the media). Thus, the cellulose is cultivated at the liquid-air interface. When the bacteria and media are enclosed in a gas-permeable membrane, the bacteria will migrate to the boundary where air can be obtained. The cellulose is then produced at the membrane boundary and is formed in the shape of the mold (53). Klemm et al. have patented a technique in which the bacteria fabricate the cellulose into hollow tubes (48). Macroscopic shaping can also be easily accomplished at the end of culture by cutting.

Additional culturing methods have been developed that improve the mechanical properties of the cellulose. The mechanical properties of biomaterials must be able to be varied so that it can be used in different applications. Adding a cell-division inhibitor to the bacteria culture produces cellulose with a greater elastic modulus (56). The patent used *Acteobacter pasteurianus* for this study. Agents, such as chloramphenicol or nalidixic acid, cause the shape of the bacterium to lengthen 2-4 times its original size of 1 μm. It also causes the cell's secretion ports to narrow in shape. This allows the bacteria to produce cellulose fibrils that are much thinner and longer than typical fibrils. The smaller microfibrils and increased hydrogen bonding causes the greater elastic modulus (56).

1.3.4.b Cellulose Modifications to Improve Mechanical Properties

Once synthesized, many other techniques can be used to alter the mechanical and chemical properties of bacterial cellulose. Extensive purification via alkaline and oxidative agents increases the Young's Modulus of the bacterial cellulose (54). These treatments remove impurities in the cellulose matrix, namely proteins and nucleic acids from the bacteria and media remaining after culture. Yamanaka et al. proposed that removing the non-cellulosic components increases the contact between the cellulose fibrils which permits more intra-and interfibrillar hydrogen bonds (54).

Another study showed that drawing the cellulose uniaxially also improves its mechanical properties (57). Cellulose samples were stretched in the hydrated state and then air-dried without releasing the strain. After being stretched at 15% strain, the tensile strength increased from 197 MPa to 337 MPa. The elastic modulus also increased from 11.1 GPa to 33.5 GPa. Crystallite orientation was determined by measuring x-ray pole figures on a SIEMENS texture goniometer. Once stretched, it was seen that the cellulose fibrils increased in planar orientation. These results indicate that fibril orientation has a great effect on the mechanical properties of bacterial cellulose (57).

Oxidizing cellulose makes it more resistant to bacterial growth. Oxidized cellulose is also more degradable in the body. Oxidation causes the pyranose ring of the cellulose to open and form dialdehyde cellulose (Figure 1.7, following page). Due to the opened ring, dialdehyde cellulose can be broken down into carboxylic groups, primary alcohols, or imines with primary amines (58). The degradation time can be controlled by varying the amount of oxidation.

1.3.4.c Cellulose Modifications to Improve Chemical Properties

Cellulose chemistry has been studied for over 200 years. Various methods have been developed to alter and modify this polymer (60). Hydroxyl groups comprise 31.5% of cellulose by weight (61). Hydroxyl groups enable addition, substitution, and oxidation reactions. Cellulose derivatives can be made by etherifcation, esterification, cross-linking, or graft-copolymerization (61).

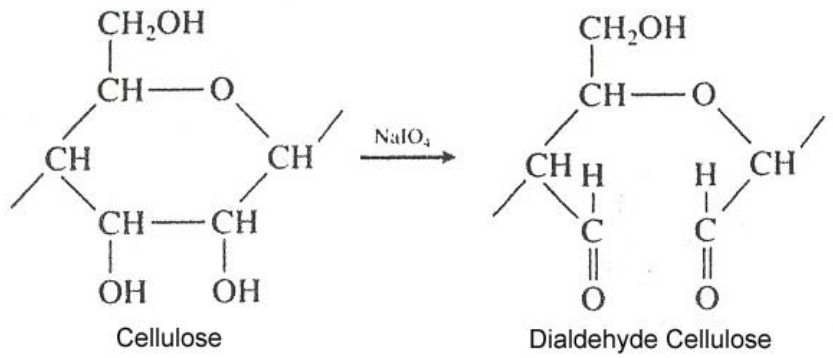

Figure 1.7: Periodate Oxidation of Cellulose

Cellulose treated with sodium periodate to make Dialdehyde Cellulose

(59)

Esterification reactions produce derivatives such as cellulose acetate, cellulose acetate-butyrate, cellulose acetate-phthalate, and cellulose phosphate. Cellulose acetate has shown promise for the controlled release of steroids for medical applications. Cellulose acetate-butyrate has been used in preparation of progesterone microspheres, enteric coating applications, and has been investigated for use in hard contact lenses. Cellulose phthalate has been used to coat specific tablets that resist acids in the stomach but readily dissolve in the intestine (61).

Etherification produces methylcellulose, hydroxyethylcellulose, hydroxypropylcellulose, hyroxypropylmethylcellulose, and sodium carboxymethylcellulose. Hydroxyethylcellulose is used in tablets and lozenges while hydroxypropylcellulose is used to coat pharmaceutical tablets. Both hyroxypropylmethylcellulose and sodium carboxymethylcellulose are used as a thickening agent, a tablet excipient, and a laxative (61).

Proteins can also be added onto the hydroxyl groups to enhance biocompatibility. Incorporating physiological proteins such as fibronectin, osteopontin, or osteonectin may facilitate bone cell attachment. The arginine, glycine, and aspartic acid peptide sequence (RGD) is found

in many adhesion proteins in the body. When grafted onto polymers, the RGD sequence has found success in promoting cell adherence (62). Aspartic acid, glutamic acid, and serine are a peptide sequence suspected to control the mineralization of bone (63). Attaching them to cellulose may enhance bone ingrowth.

1.3.4.d Phosphorylation to Promote Mineralization

Natural collagen has a strong affinity for binding phosphate ions. These localized sites proceed to bind with calcium to form apatite. Cellulose can likewise contain phosphate groups. They can be added by chemical phosphorylation. Phosphorylation attaches phosphate groups to the hydroxyl ends of the cellulose by esterification (Figure 1.8). The presence of this functional group enables the cellulose to bind with calcium ions to form calcium phosphate particles. Phosphorylated chitin and cotton (plant cellulose) enable the deposition of hydroxyapatite particles onto their respective fibrils when immersed in simulated body fluid (33). In in-vivo studies, it was seen that implanted cellulose phosphates produced a calcium phosphate layer (36). This mineral layer could induce satisfactory bone bonding between cellulose and host tissue.

1.3.5 Bacterial Cellulose as a Biomaterial

Because 99.8% of the cellulose mass is water, and the 0.2% cellulose that is present is an inert polysaccharide, bacterial cellulose has is relatively pure. Though it is lightweight, the

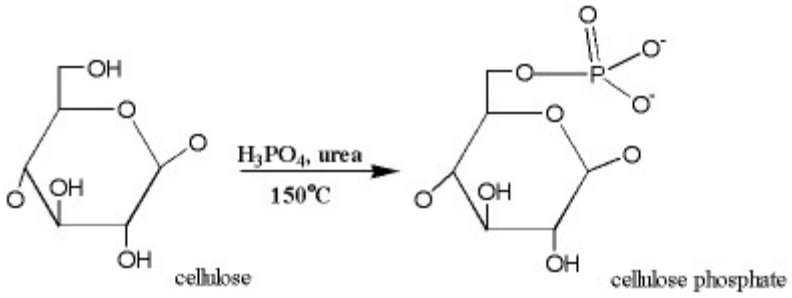

Figure 1.8: Phosphorylation of Cellulose

Image created on ChemDraw®

crystalline microfibrils give BC high tensile strength. It is also moldable and has excellent shape retention (53).

The crystalline structure of bacterial cellulose also gives it extraordinary water capacity, with a retention value of ~1000% (48). Because it is highly hydrated and porous like living tissue, it allows the permeation of water and waste products. Because cellulose is a hydrogel, it is also susceptible to calcification, enabling it to be used a bone precursor (64).

The β-1,4 linkages of cellulose are not easily broken once it is implanted in the body. Humans lack a cellulase enzyme that enables the digestion of cellulose. This indicates that cellulose could be used for long-term implantation if used in its native state. However, chemical modifications such as oxidation permits cellulose to degrade faster than native cellulose.

In 1995, the FDA approved use of a skin substitute called Biofill®. Biofill® consists of a dried bacterial cellulose barrier which allows the permeation of gas and vapor, but not liquid. It has been successfully used to treat burns, ulcers, and lacerations (65). As mentioned previously, an American company called Xylos Corporation also manufactures bacterial cellulose wound dressings.

Another product being developed is Gengiflex®. This product is similar to Biofill®, except it contains an external layer of alkali-treated bacterial cellulose bonded to an internal layer of crystalline bacterial cellulose. In a paper published by Novaes et al, Gengiflex® was shown to heal canine gingival lesions caused by periodontis. It has yet to be manufactured and approved for human periodontal regeneration (66).

A second product with favorable animal testing results is BASYC®. BASYC® consists of cellulose that has been directly synthesized into hollow tubes by using gas permeable molds. Used as vessel replacements, the tubes were implanted into rat carotid arteries. They had a 100% patency rate with no signs of coagulation or proliferation after a four week period. The tubes became wrapped in connective tissue. The inner layer became lined with endothelial cells which were identified using an immunohistochemical method based on an antigene-antibody reaction. A “regular vascular wall” formed within the cellulose tubes (48).

Another study achieved success in substituting bacterial cellulose for the dura mater in dogs (64). It was also proven to be a functioning substrate for mammalian cell culture (68). In addition, bacterial cellulose membranes have been used to build glucose sensors for diabetic patients (69).

1.4 Techniques from Previous Studies

In an investigation by Serafica et al., solid particles were incorporated into bacterial cellulose by a different technique than the one presented in this thesis (70). In the prior study, the cellulose was cultured in a rotating disk reactor. Particles were added to the culture as a concentrated slurry . A circulation system was incorporated into the reactor to prevent the particles from settling before incorporation. Small aluminum, iron, sephadex, silica, and calcium carbonate particles were incorporated into the bacterial cellulose during culture in the disk reactor (70).

Evans et al. demonstrated that palladium particles could be incorporated into bacterial cellulose (71). Bacterial cellulose was incubated in ammonium hexachloropalladate dissolved in 50 mM sodium acetate at 38°C. This produced a homogenous layer of palladium throughout the matrix. The catalytic layer was capable of generating hydrogen when incubated with sodium dithonite indicating its potential application in electrochemical systems (71).

Other studies have attempted to deposit apatite onto plant cellulose fibers (72, 73, 74). Yokogawa et al. phosphorylated commercial cellulose fibers derived from plants (72). They first incubated the phosphorylated cellulose in calcium hydroxide and then in simulated body fluid. After 9 days of incubating in simulated body fluid, an apatite formed with a Ca:P ratio of about 1.67 (indicative of hydroxyapatite) (72). Granja et al. utilized regenerated cellulose from the viscose process (73). The regenerated cellulose was phosphorylated, incubated in 50 mM calcium chloride for 24 hours, and then incubated in simulated body fluid for 15 days. Calcium phosphate salt formed with a Ca:P ratio of 1.66 (73).

Rhee et al. incubated cellulose cloth derived from plants in citric acid followed by

incubation in simulated body fluid (74). Tiny crystals formed on the surface of the cloth, and x-ray diffraction confirmed that the crystals were hydroxyapatite. FTIR indicated that the HAP may have been attaching via hydrogen bonding. This implies that the crystals are susceptible to detachment due to the weak bond strength (74).

1.5 Potential use in Bone Tissue Engineering

It is hoped the calcium deficient hydroxyapatite-bacterial cellulose composite may find use as an orthopedic biomaterial. Bone is the second most implanted material next to blood (4). Musculoskeletal pathologies cost the U.S. economy an estimated $215 billion a year (75) causing bone grafts to have a market potential of $400 to $600 million per year (18).

Though autografting and allografting remain the two primary sources for bone grafts, there are many shortcomings associated with these techniques. Autografting requires a painful second surgery for bone harvesting and the supply of useful bone is limited. Allografting exposes the patient to higher risk for infection and other diseases. It is also very costly and limited due to the shortage of bone banks (76).

Bone tissue engineering is one of the most promising technologies for bone substitution. This entails the use of a scaffolding material to either induce formation of bone from the surrounding tissue (acellular) or to act as a carrier or template for implanted bone cells (cellular). Acellular constructs can be solid absorbable fillers that degrade over time, or porous scaffolds that allow bone ingrowth (77). The cellular tissue engineering process entails the extraction of osteoblasts and mesenchymal stem cells from the patient, proliferating them in culture, seeding them onto a suitable scaffold, and implanting the cell-seeded scaffold back into the patient. As the tissue structures grow into the implant, the scaffold will slowly degrade and resorb (78). Choosing the right scaffold material is vital to the success of tissue engineering. It must be highly biocompatible and sterilizable, enable cell attachment and proliferation, be porous enough to support bone growth, able to degrade and resorb as the tissue populates the construct, adaptable to an irregular wound site, and have the correct mechanical and physical properties for the application (77).

The calcium-deficient hydroxyapatite-bacterial cellulose composite possesses many of these properties. The biocompatibility of bacterial cellulose (48, 65, 66, 67) and calcium deficient hydroxyapatite (19, 30) has been shown in many studies. Cell attachment and proliferation on bacterial cellulose has also been proven (68). Bone ingrowth in plant viscose cellulose was verified by Martsen et al. (79). Chemically modifying the cellulose allows its degradability to be controlled. Cellulose can be shaped either during synthesis (53), or by cutting after synthesis. The presence of calcium-deficient hydroxyapatite should promote secure bonding with bone (19).

Cellulose, like other polysaccharides, is an excellent drug-carrying device (41). CdHAP also facilitates the loading of therapeutic agents (19). This permits the composite to carry additional pharmaceuticals that would promote healing and suppress inflammation. The structure of cellulose facilitates the addition of proteins onto its hydroxyl groups. Bone morphogenetic proteins (BMPs) have shown remarkable success in inducing bone formation and repair when associated with bone tissue engineering scaffolds. Adding BMPs to cellulose can enhance its performance as a bone substitute (77).

The CdHAP-BC composite may also find use as a dental biomaterial since teeth share many of the same characteristics as bone. One of the current strategies in dental restoration is the use of hybridized materials, or materials associated with a polymeric material (78). However, dental materials are usually designed to be permanent and must be resistant to demineralization and degradation (80). This means a more stoichiometric HAP containing fluoride ions would have to be synthesized; and the cellulose must be treated to resist degradation.

Chapter 2

Materials and Methods

2.1 Bacterial Cellulose

2.1.1 Commercial Source of Bacterial Cellulose

Nata de coco, or coconut gel, is a Filipino food product consisting of bacterial cellulose grown from fermented coconut milk. After the cellulose is washed, it is cut into cubes and preserved in sugar syrup. Many brands of nata de coco, such as Islands' Best Cocogel (RFM Corporation, Manila, Philippines) or Coconut Gel (Jo-na's International Philippines Incorporated, Quezon City, Philippines) can be obtained in the U.S. Though nata de coco cubes were not used in this study, they can be used as a source of bacterial cellulose for scientific experiments. Cubes are washed extensively with water, 1% sodium hydroxide, 500 mM sodium acetate, and undergo a final wash with water prior to use.

2.1.2 Cultivation of Bacterial Cellulose from Gluconacetobacter hansenii

For the present study, the bacterial strain *Gluconacetobacter hansenii (G. hansenii)* was obtained from the American Type Culture Collection (Manassas, VA) (ATCC 10821) to synthesize bacterial cellulose.

The bacteria were cultivated on Schramm-Hestrin Media, developed by Schramm and Hestrin in 1954 (50). This nutritional broth is made by combining the reagents listed in Table 2.1. The reagents were dissolved in distilled water, the volume was brought up to one liter, and the pH was adjusted to 6.0 with the addition of hydrochloric acid or sodium hydroxide. The media was

Table 2.1: Reagents used in Schramm-Hestrin Medium

Reagent	Amount
Glucose	20 g
Yeast Extract	5 g
Peptone	5 g
Sodium Phosphate Dibasic	2.7 g
Citric Acid	1.15 g
Distilled Water	1 L

(50)

then autoclaved at 121°C for 20 minutes. Other types of sugars, such as fructose or mannitol, were used instead of glucose in some formulations.

A synthetic medium was also used in certain experiments which does not contain the yeast and bactopeptone ingredients. This media was developed by Cannon and Anderson (55). All the reagents in Table 2.2, excluding the niacinamide, thiamine, and calcium pantothenate; were combined. The volume was brought up one-liter and autoclaved for 20 minutes at 121°C. The niacinamide, thiamine, and calcium pantothenate were filter- sterilized and added to the sterilized media after cooling to room temperature. Cellulose cultured in synthetic media generally grows slower, and are usually more transparent and thinner than cellulose grown in rich media. However, cellulose grown on synthetic media is easier to purify since there are fewer complex proteins to remove following pellicle formation.

The bacteria were maintained on Mannitol 1 Agar as recommended by ATCC. The reagents in Table 2.3 (following page) are dissolved in water, and brought to a 1-L volume. The mixture was then autoclaved at 121°C for 15 minutes and poured into culture dishes. A preculture was then streaked onto the agar plates with bacterial inoculation loops. Without

Table 2.2: Reagents used in Synthetic Medium

Reagent	Amount
Glucose	10 g
Ammonium Chloride	1 g
Citric Acid	1.15 g
Sodium Phosphate Dibasic	3.3 g
Potassium Chloride	0.1 g
Magnesium Sulfate Heptahydrate	0.25 g
Niacinamide	100 mg
Thiamine	100 mg
Calcium Pantothenate	100 mg
Distilled Water	1 L

(55)

Table 2.3: Reagents used in ATCC Mannitol 1 Agar

Reagent	Amount
Yeast Extract	5 g
Peptone	3 g
Mannitol	15 g
Agar	15 g
Distilled Water	1 L

Protocol from http://www.atcc.org/mediapdfs/1.pdf

further maintenance, colonies began to form on the agar within a few days. New precultures were made by removing a single colony from the agar plates, placing it in Schramm-Hestrin Media, and allowing it to culture under agitated conditions provided by an orbital shaker.

For synthesis of cellulose pellicles, a seed culture of *G. hansenii* was grown in Schramm-Hestrin medium in a flask under agitated conditions. After 2-3 days of preculture, the seed culture was diluted in a 1:10 ratio with the prepared Schramm-Hestrin media. The diluted culture was then transferred to sterile 6 or 10 cm diameter culture dishes. The culture was kept at room temperature (~23°C). The cellulose was then harvested 2 weeks after culture. Cultivation time can vary depending on the desired thickness. "Harvesting" consists of lifting the pellicle off the liquid surface with forceps.

2.1.3 Purification of Bacterial Cellulose

After harvesting, the cellulose pellicle was placed in a beaker of distilled water, put into a water bath, and heated to 90°C for 1-2 hours to kill the bacteria. The pellicles were then rinsed with distilled water, and treated with a purifying agent to remove bacterial debris and growth media components. Different chemicals were tested to determine which optimally purified the cellulose. Sodium dodecyl sulfate (SDS), sodium hydroxide (NaOH), and mixtures of SDS and NaOH were evaluated. The difficulty of removing the SDS after purification resulted in the selection of sodium hydroxide as the purifying agent.

The pellicles were incubated in 1% NaOH under agitated conditions at room temperature (23°C) for 1-7 days. Every 24 hours, the NaOH was decanted and fresh solution was added.

Polypeptides and DNA left in the bacterial cellulose after cultivation absorb in the UV region. Their presence in the used sodium hydroxide solution indicated the purity of the bacterial cellulose. The absorbance at 280 nm was read on Carey50 Spectrophotometer (Varian, Palo Alto CA). A high absorbance indicated that the NaOH had removed a great deal of impurities. As the absorbance decreased, it was assumed that less proteins and nucleic acids remained in the cellulose. An absorbance reading of approximately 0.05 - 0.10 signified that enough debris had been removed to deem the cellulose pure.

After the sodium hydroxide treatment, the cellulose was soaked in several changes of nanopure water to neutralize the NaOH in the cellulose. The washings continued until the pH was near neutrality (pH ~7). The cellulose can either be stored in distilled water under refrigeration (5-10°C) or in 20% ethanol to prevent contamination.

2.2 Methods of Mineral Deposition

2.2.1 Precipitation of Calcium Phosphate

A BC pellicle was placed in 100mM $CaCl_2$ (pH 4.83) for 24 hours. It was then briefly rinsed with nanopure water, and incubated in 60mM Na_2HPO_4 (pH 8.36) for a further 24 hours. This cycle was repeated two more times for a total of 3 daily soakings of 100mM $CaCl_2$ alternated with 3 daily soakings of 60mM Na_2HPO_4. All incubations were carried out at 23°C.

The effect of varying the number of solution cycles on the amount of calcium phosphate incorporated was examined. Four 10 cm (diameter) samples of identical BC pellicles were synthesized under identical conditions. The cellulose was grown on 2% Schramm-Hestrin Fructose Media for 9 days. The cellulose was purified with SDS for 3 days, and purified with nanopure water for 2 days. One pellicle was incubated in 3 cycles of subsequent incubations of calcium and phosphate solutions, another underwent 4 cycles of incubations, and a third went through 5 cycles of incubations. The last pellicle was stored in water as a control.

Increasing the molarity of the calcium chloride and sodium phosphate dibasic solutions was also investigated. Ten additional 10 cm (diameter) bacterial cellulose pellicles were synthesized under identical conditions. The cellulose was grown on 2% Schramm-Hestrin

Fructose Media for 11 days. The cellulose was purified with SDS for 3 days, and purified with nanopure water for 2 days. Two of the pellicles were stored in water as controls. Each of the other 8 pellicles underwent 2 cycles of $CaCl_2$/Na_2HPO_4, as described above. The concentration of the $CaCl_2$ and Na_2HPO_4 were varied for each pellicle but the molar ratio of Ca to P was kept to 10:6 for each sample to mimic the Ca:P concentration of hydroxyapatite. All reactions were carried out at 23°C. The concentrations of calcium chloride ranged from 25mM to 200mM, and the sodium phosphate dibasic concentrations varied from 15mM to 120mM.

Other salt solutions were investigated for use as calcium and phosphate ion donors. The cellulose was incubated in 12mM $Ca(OH)_2$ (calcium hydroxide) and 60mM Na_2HPO_4, 100mM $CaCl_2$ and K_2HPO_4 (potassium phosphate dibasic), and 100mM $CaCl_2$ and 60mM $Na_5P_3O_{10}$ (sodium tripolyphosphate) with alternating cycles.

All of the treated pellicles were briefly rinsed in nanopure water to eliminate unincorporated salts before being put on a gel-dryer (Drygel Jr., Model SE540, Hoefer Scientific Instruments) for 30 minutes at 80C. The samples were weighed and the thicknesses were measured to determine the amount of calcium phosphate precipitated. A micrometer (Mitutoyo 103-125) was used to measure the thickness of the dried treated pellicles.

2.2.2 Preparation of Simulated Physiological Fluid

Simulated body fluid (SBF) was prepared from a protocol developed by Tas (12). The reagents listed in Table 2.4 (following page) were dissolved in nanopure water and brought up to a one liter volume. It was then heated to 37°C (physiological body temperature) via a water bath and titrated to pH 7.40 with 1M HCl. The solution was either immediately used or stored at 5-10°C. The SBF was discarded once precipitation in the solution occurred.

2.2.3 Incubation in Simulated Physiological Fluid

Eight bacterial cellulose pellicles were synthesized under identical conditions as described above. Two samples of cellulose were reserved as control. Two samples of cellulose were incubated in SBF for 11 days. The SBF was exchanged with fresh solution every second day. Two samples underwent calcium phosphate precipitation by the protocol previously

Table 2.4: Reagents used in Simulated Body Fluid

Reagent	Amount
NaCl	6.547 g
$NaHCO_3$	2.268 g
KCl	0.373 g
$Na_2HPO_4 \bullet 2H_2O$	0.178 g
$MgCl_2 \bullet 6H_2O$	0.305 g
$CaCl_2 \bullet 2H_2O$	0.368 g
Na_2SO_4	0.071 g
$(CH_2OH)_3CNH_2$	6.057 g
Distilled Water	1 L

(12)

described. Two more samples underwent calcium phosphate precipitation, and then were incubated in SBF for 11 days with fresh solution added every second day. The last two samples were kept in nanopure water for control. All incubations were carried out at 23°C. The samples were then put on a gel dryer for 30 minutes at 80°C and weighed. The thickness of the dried pellicles was measured using a micrometer (Mitutoyo 103-125).

2.2.4 Phosphorylation of Bacterial Cellulose

Bacterial cellulose pellicles were phosphorylated based on the method described by Head et al. (81). First, the volume of water in the purified bacterial cellulose was estimated by weight. Due to the density of water, a 1.0 g weight is equivalent to a 1.0 mL volume. The cellulose was then equilibrated with 45% urea (by weight) for 24 hours. The total concentration of urea in the cellulose was estimated based on its volume and the concentration of urea. It was then equilibrated with another volume of 45% urea for 24 hours. The total concentration of cellulose was estimated again. The pellicles were then equilibrated with a 42% phosphoric acid/75% urea solution at room temperature for 24 hours. The final concentration of cellulose was then estimated. Target values of concentration were approximately 30-35% phosphoric acid and 50-55% urea. The treated cellulose was then placed in an oven at 120°C for 3 hours. They were then rinsed extensively with nanopure water.

The ion exchange capacity of the cellulose was measured to quantify the extent of phosphorylation. A phosphorylated cellulose pellicle weighing 0.161 g was used for this analysis. The pellicle was placed in 0.5M sulfuric acid for four hours to protonate the phosphate groups. The excess acid was removed by washing extensively with nanopure water. The modified pellicle was then boiled in H_2O and deaerated under vacuum at room temperature to remove carbon dioxide gas that would interfere with the titration. The cellulose was then placed in 100 mL of nanopure water and titrated against a standard 32.4 mM NaOH solution. Aliquots of NaOH were added and the pH values were recorded after 20-30 minutes when the pH equilibrated.

2.2.5 Precipitation of Apatite in Phosphorylated Bacterial Cellulose

Five phosphorylated bacterial cellulose pellicles were synthesized under identical solutions. The phosphorylated BC pellicles were incubated in various calcium solutions to determine if apatite precipitation would occur. One phosphorylated bacterial cellulose pellicle was incubated in 100 mM $CaCl_2$ for 14 days with fresh solution added every second day. Another phosphorylated bacterial cellulose pellicle was incubated in saturated calcium hydroxide (12mM) for 14 days with fresh solution added every other day. A third phosphorylated sample was incubated in 12 mM calcium hydroxide for 9 days with fresh solution added every other day. Subsequently, the sample was then incubated in simulated body fluid for 9 days with fresh solution added every other day. A fourth phosphorylated sample was incubated in 100 mM calcium chloride for 9 days with fresh solution added every other day. Subsequently, the sample was then incubated in simulated body fluid for 9 days with fresh solution added every other day. The last phosphorylated pellicle was stored in water as a control.

All incubations were carried out at 23°C. Samples were placed on a gel-dryer for 30 minutes at 80°C, weighed for analysis, and measured for thickness. Additional analyses on the processed samples are discussed below.

2.2.6 Inclusion of Fluoride and Carbonate Ions

The precipitation mechanism of alternating salt solution incubations was also attempted using calcium chloride with potassium fluoride and sodium carbonate.

Bacterial cellulose pellicles synthesized under identical conditions were utilized. One bacterial cellulose pellicle was placed in 100mM $CaCl_2$ for 24 hours. It was then briefly rinsed with nanopure water, and then incubated in 200mM potassium chloride (KF) for a further 24 hours. This cycle was repeated two more times for a total of 3 daily soakings of 100mM $CaCl_2$ alternated with 3 daily soakings of 200mM KF. All incubations were carried out at 23°C.

A second bacterial cellulose pellicle was placed in 100mM $CaCl_2$ for 24 hours. It was then briefly rinsed with nanopure water, and then incubated in of 100mM sodium carbonate (Na_2CO_3) for a further 24 hours. This cycle was repeated two more times for a total of 3 daily soakings of 100mM $CaCl_2$ alternated with 3 daily soakings of 100mM Na_2CO_3. All incubations were carried out at 23°C. Again, the analysis of the samples are discussed below.

2.3 Analysis of Mineral Deposition

2.3.1 Alizarin Red S Staining

Alizarin Red S, a dye commonly used to identify calcium in histology, was also employed to indicate calcium incorporation in the bacterial cellulose. Samples were stained with 2% Alizarin Red Solution (Sigma), and rinsed with repeated washes of nanopure water. Presence of calcium was indicated by a red color and evaluated visually.

2.3.2 Laser Induced Breakdown Spectroscopy

Proof of calcium and phosphate induction into the matrix was first confirmed using Laser Induced Breakdown Spectroscopy. Four samples were evaluated: a gel-dried sample of the calcium phosphate cellulose, a freeze-dried sample of the calcium phosphate cellulose, a gel-dried sample of unaltered cellulose, and a freeze-dried sample of unaltered cellulose. Each sample was derived from the same 10 x 8 x 0.3 cm bacterial cellulose (wet weight 79.8 g) cut into 4 approximately equal pieces. The laser used was a Spectra Physics pulsed Nd:YAG laser (Model INDI-SHG-50) with a fundamental wavelength of 1064 nm. The frequency was doubled to give an output wavelength of 532 nm, and the frequency was quadrupled to give a 266 nm wavelength. The spectrometer was a 0.5 m Acton spectrometer (Model SP 500) which had a resolution of 0.05 nm.

2.3.3 X-Ray Diffraction

X-Ray Diffraction (XRD) analysis was performed on a precipitated cellulose pellicle after 2 cycles of incubations in 100mM calcium chloride solution and 60mM Na_2HPO_4. Dried unmodified bacterial cellulose was also evaluated. The dry weights of the calcium phosphate bacterial cellulose and the unaltered bacterial cellulose were 191 mg and 40 mg respectively. The measurements were made with a Siemens D5005 X-Ray Diffraction Machine. The sample was run with a step-scanning mode of 2θ=15.0° and a count time of 20 s. The Cu Kα tube operated at 40kV and 20 mA.

X-ray diffraction was also performed on native bacterial cellulose and phosphorylated bacterial cellulose incubated in various salt solutions. Diffraction patterns from native bacterial cellulose incubated in simulated body fluid, incubated in $CaCl_2$ and SBF, incubated in $Ca(OH)_2$ and SBF, incubated in $CaCl_2$ and KF, and incubated in $CaCl_2$ and Na_2CO_3 were acquired. Also, diffraction patterns from the phosphorylated cellulose incubated in SBF, $CaCl_2$, $CaCl_2$ and SBF, $Ca(OH)_2$, and $Ca(OH)_2$ and SBF were acquired. A Scintag XDS2000 Room Temperature X-Ray Diffractometer was used with Cu Kα radiation operated at 40kV and 20mA. A 10-70 2θ scan was collected at a 1 per minute scan rate.

2.4 Mammalian Cell Culture Testing

2.4.1 Reviving Osteoblast Culture

In-vitro studies were carried out with a cell line obtained from the American Type Culture Collection (ATCC CRL-2594). MC3T3-E1 Subclone 14 is an osteoblast line derived from mouse calvarium. A frozen 1mL ampule of passage number 16 containing 2.9 x 10^6 cells per milliliter was acquired from ATCC. The package information stated that the cells were from passage 16, meaning that the cells had been subcultivated 16 times since the initial cell line was acquired. As the cell line is further subcultivated, the passage number increases by one. The frozen ampule was immediately revived upon receipt.

Before reviving the culture, an appropriate nutritional medium was made to maintain the cells. The medium consisted of 90% Alpha Minimum Essential Medium Eagle (αMEM) (Sigma)

which contains ribonucleosides, deoxyribonucleosides, and sodium bicarbonate. It was combined with Fetal Bovine Serum (FBS) in a ratio of 1:9. The medium was also nutritionally supplemented with 2mM L-glutamine and 2mM sodium pyruvate. The complete αMEM medium was warmed in a 37°C water bath prior to use.

10mL of complete αMEM medium was pipetted into a 10 cm culture dish, and placed in a 37°C / 5% CO_2 incubator to warm. The frozen ampule was placed in a 37°C water bath and agitated for approximately 3 minutes until the contents were completely thawed. The 10 cm dish with the warmed media was removed from the incubator, and the 1 mL of thawed cell culture was pipetted into the dish (passage 17). The dish was placed in the 37°C / 5% CO_2 incubator.

2.4.2 Expanding the Cell Line

To accumulate an appropriate supply of osteoblasts to perform the in-vitro studies, the cells were cultured and expanded. After 2 days, passage 17 grew to a thick monolayer. The initial media was removed from the culture dish, the cells were rinsed 1 mL of Phosphate Buffered Saline (PBS), and ½ mL of Trypsin/EDTA (Sigma) was added to the monolayer. The dish was placed in a 37°C / 5% CO_2 incubator for 2-3 minutes. Once cell detachment was observed via a light microscope, 5 mL of fresh complete αMEM medium was added to the trypsinized cells. The cells and medium were aspirated by pipetting, and 1 mL of the cell media were added to 5 culture dishes (10 cm diameter) that contained 10 mL of complete αMEM medium (passage 18).

2.4.3 Long Term Storage of Cell Line

At 3 days of cultivation, the initial media was removed and 10 mL of fresh media was added to each of the 5 dishes of passage 18. At 5 days of cultivation, 3 of the 5 dishes of passage 18 were removed from the incubator. The media was removed, the cells were rinsed with 1 mL of PBS, and detached from each dish by adding ½ mL of trypsin. Each set of cells were resuspended in 4 mL of complete αMEM medium and aspirated by pipetting. The cell suspension was centrifuged at 1000 rpm for 5 minutes. The supernatant was removed, and the cells were combined with 10 mL complete αMEM medium that contained 10% dimethyl sulfoxide

(DMSO, a cryoprotectant) and aspirated by pipetting. The suspension was pipetted in 2 mL aliquots into 5 vials. The vials were placed in a dewar of liquid nitrogen for 30 minutes. The vials were then placed in a cryogenic storage dewar.

2.4.4 Cell Counts

Viability of the osteoblast population was measured by counting the cells with the aid of Trypan Blue (Sigma) and a hemocytometer. The cells were diluted in a 1:10 ratio with media. One mL of Trypan Blue was added to the cell suspension and aspirated by pipetting. The trypan blue stains non-viable cells blue. One drop of the stained cell suspension was placed under the cover slip of a hemocytometer. The hemacytometer is a glass chamber that is etched with a grid. It holds the cover slip 0.1 mm above the chamber floor. The hemacytometer contains a large square (0.1 cm x 0.1 cm) that has a volume of 0.0001 mL. The large square is divided into 16 squares for easier counting. The hemacytometer is viewed under a light microscope at 100x magnification. The viable cells (non-blue) are counted in the 16 square area (0.1 cm x 0.1 cm). This number x 10^4 was the number of cells per mL of the tested cell population.

2.4.5 Crystal Violet Staining

To observe the osteoblasts more clearly on the cellulose substrates, they were stained with Crystal Violet. First, the cell-attached pellicles were washed with PBS. Ten mL of methanol was then pipetted onto the pellicle and left to sit for 5 minutes. Then 10 mL of Crystal Violet stain was added to the cellulose and incubated for 10 minutes. The stain solution was then removed by pipetting, and the pellicles were rinsed in repeated washes of water.

2.4.6 Alkaline Phosphatase Assay

To determine the viability of the osteoblasts, an alkaline phosphatase assay was performed on the cell samples. The protocol for this assay was taken from Lowry et. al (82) and Hakeda et. al (83). The cells were suspended in complete αMEM medium and rinsed with two washes of phosphate buffered saline. After washing, osteoblasts were resuspended in 1 mL of 0.2% Nonidet P.40 in a conical tube. The tube containing the cell suspension was then placed in an ice bath and the cells lysed by sonication for 1 minute. The lysed cells were then centrifuged

at 2500g for 10 minutes to separate the supernatant from the cell fragments. The supernatant was reserved, and the pellet containing cell fragments was discarded.

Alkaline phosphatase (ALP) is a natural enzyme found in osteoblasts. ALP hydrolyzes esters and anhydrides of phosphate (H_3PO_4). The amount of ALP present in the osteoblasts was measured by combining the cell lysate with p-nitrophenyl phosphate. ALP causes p-nitrophenyl to liberate p-nitrophenol by hydrolysis (Figure 2.1). p-nitrophenol is yellow and absorbs at 410 nm. The absorbance of the color increases as more p-nitrophenyl phosphate is converted to p-nitrophenol.

A buffer for the p-nitrophenyl phosphate was made with 0.56 M 1-amino-2-methyl-1-propanol and 1 mM $MgCl_2$. A reagent mixture was made with by making a 10 mM solution of p-nitrophenyl phosphate in the buffer. A cuvette with the reagent mixture that had been heated to 37°C in a water bath was placed in a spectrophotometer to "zero" the scan. Subsequently, a cuvette containing 800 µL of the reagent mixture was heated to 37°C in a water bath before adding 200 µL of the cell lysate. An enzyme kinetic scan was performed at 410 nm for 10 minutes. The reaction was stopped by adding 2 mL of 0.25 M NaOH to the cuvette. The final absorbance was then read at 410 nm.

2.4.7 In-Vitro Testing of Native Bacterial Cellulose Vs. Calcium Phosphate Bacterial Cellulose

Mammalian cell culture tests were conducted with native bacterial cellulose and calcium phosphate bacterial cellulose to determine if the cells would attach and proliferate on the

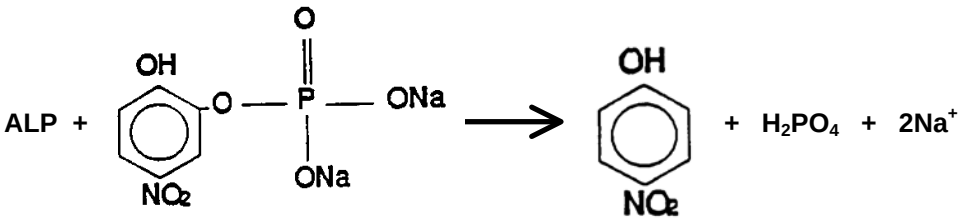

Figure 2.1: Liberation of p-Nitrophenol from p-Nitrophenyl Phosphate Reacted with Alkaline Phosphatase

Image created on ChemDraw®

substrates. Two pellicles of native bacterial cellulose and 2 pellicles of bacterial cellulose precipitated with calcium phosphate were utilized. All four cellulose samples were 6 cm in diameter and synthesized under identical conditions. They were grown on 2% Fructose Schramm-Hestrin Medium for 28 days. They were then purified with daily treatments of 1% SDS/1% NaOH for 7 days. They were neutralized with daily treatments of nanopure water for 14 days. Two of the cellulose samples were then incubated in 3 alternating daily cycles of 100 mM $CaCl_2$ and 60 mM Na_2HPO_4. The two unaltered bacterial cellulose samples are referred to as UABC I (unaltered bacterial cellulose), UABC II, CPBC I (calcium phosphate bacterial cellulose), and CPBC II. The cellulose samples were placed in phosphate buffered saline and autoclaved for 20 minutes at 121°C.

Five dishes of the MC3T3-E1 cell line from passage 21 were utilized after 11 days of cultivation with fresh media added on the 4^{th} day. A healthy monolayer was observed in each culture dish. Each of the dishes was resuspended separately. Four of the five cell suspensions were used for seeding each of the four samples. The last cell suspension was placed back into a fresh culture dish to be used as a control.

The media was removed from each culture dish by pipetting, the cells were rinsed with PBS, and then treated with 0.5 mL of trypsin. Following detachment, 9.5 mL of complete αMEM medium was added to each dish to neutralize the trypsin. Each cell suspension was then transferred to a 15 mL conical tube. The suspensions were centrifuged at 1000 rpm for 5 minutes. The medium was extracted, and 4.5 mL of complete αMEM medium was added and aspirated by pipetting. One mL of each cell suspension was stained with Trypan Blue and counted on a hemocytometer.

Prior to seeding, the cellulose pellicles were incubated in 10 mL of media for 30 minutes in a 37°C / 5% CO_2 incubator. The media was then removed. Two mL of cell suspension was aliquoted to one side of each pellicle, and then placed in the incubator for 10 minutes. Then the remaining 2 mL of suspension was aliquoted to the other side, and allowed to incubate for 10 minutes. Each sample was then floated in 15 mL of complete αMEM medium and placed in the

incubator for 10 minutes. The cells were cultured on the cellulose for 10 days with fresh media added on the 5th day.

After 10 days, the media was removed from each sample; and the cellulose was separated from its original dish. Each cellulose pellicle and each of the culture dishes were treated with ½ mL of trypsin. Cell counts and an alkaline phosphatase assay was performed on each set of cells from the cellulose and the culture dishes.

2.4.8 In-Vitro Testing of Bacterial Cellulose Grown in Rich Media Vs. Synthetic Media

Three pellicles of bacterial cellulose grown on Schramm-Hestrin (rich) Medium and two bacterial cellulose pellicles grown on a synthetic medium were synthesized. 3 6-cm pellicles were grown on 2% Glucose Schramm-Hestrin Medium for 36 days. They were then purified with daily treatments of 1% NaOH for 19 days. They were neutralized with daily treatments of nanopure water for 6 days. These samples are referred to as RBC I, RBC II, and RBC III (rich bacterial cellulose). The other 2 6-cm pellicles were grown in 2% glucose synthetic medium for 28 days. They were purified with daily treatments of 1% NaOH for 19 days. They were neutralized with daily treatments of nanopure water for 5 days. These samples are referred to as SBC I and SBC III (synthetic bacterial cellulose). All five cellulose pellicles were autoclaved for 20 minutes at 121°C in phosphate buffered saline.

Six dishes of the MC3T3-E1 cell line from passage 22 were utilized after 11 days of cultivation with fresh media added on the 8th day. The cells were resuspended in the same protocol as before. The cells were seeded onto the samples in the same manner as in the previous section. One mL of the cell suspension used to seed each of the pellicles was aliquoted to a new culture dish along with 9 mL of complete media to be used as a control. The cells were cultured on the cellulose for 7 days.

After 7 days, the media was removed from each sample by pipetting. The cellulose was rinsed with phosphate buffered saline. A sample of the bacterial cellulose grown in rich media and a sample of bacterial cellulose grown on synthetic media were stained with crystal violet.

Chapter 3

Results and Discussion

3.1 Bacterial Cellulose

After the cultures were inoculated, visible clouds of cellulose began to form within one to two days. A thick "skin" of cellulose formed on the surface of the media within 5-7 days (Figure 3.1).

The *Gluconacetobacter hansenii* strain yielded a pure form of cellulose that was transparent and slippery (Figure 3.2, following page). Water composed most of the volume of the bacterial cellulose. A 1-cm thick bacterial cellulose pellicle with a 7-cm diameter and a wet weight of 39 g was placed on a gel-dryer. The cellulose reduced to a 20-μm thick film with a dry weight of 0.063 g. The pellicle contained 0.998 g of H_2O per 1.0 g of cellulose.

3.2 Deposition of Apatite

3.2.1 Cellulose in Calcium Chloride and Sodium Phosphate Dibasic

After placing the BC in the $CaCl_2$ and Na_2HPO_4 solutions, a homogenous white precipitate was found to form throughout the bacterial cellulose matrix. Deposition was immediately apparent when the BC entered the phosphate solution after incubation in aqueous calcium chloride (Figure 3.3, following page).

Figure 3.1: Synthesis of Bacterial Cellulose

Figure 3.2: Purified Bacterial Cellulose

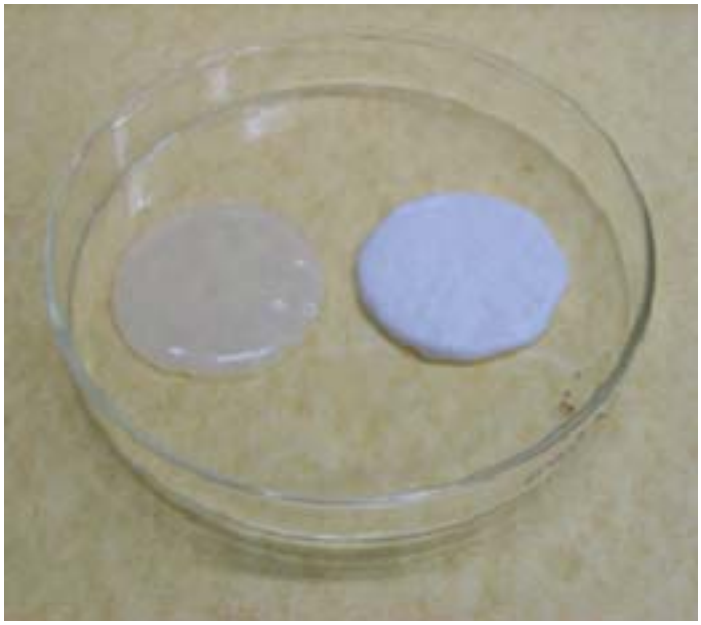

Figure 3.3: Native Cellulose and Calcium Phosphate Cellulose

Left: Native unmodified bacterial cellulose.
Right: Bacterial cellulose precipitated with calcium phosphate

Incubating the cellulose in the calcium and phosphate solutions caused an increase in thickness and rigidity. The treated cellulose and an identical sample of cellulose that had not be treated were dried, weighed, and measured for thickness. It was observed that the cellulose increased 6 ± 1 fold in weight and 17 ± 5 fold in thickness (dry weight and thickness) after being suspended in the salt solutions. The increase in weight and thickness was attributed to the apatite formed in the cellulose.

Increasing the number of times cellulose is incubated in alternating daily cycles of calcium and phosphate solution increased the amount of apatite formed in the cellulose. This was determined by weighing the pellicles after drying (Figure 3.4). It was also seen that increasing the molarity of the calcium chloride and sodium phosphate dibasic solutions increased the amount of precipitation as well (Figure 3.5, following page).

A similar deposition of white salts formed throughout the cellulose matrix after incubation in 12mM $Ca(OH)_2$ and 60mM Na_2HPO_4. Both potassium phosphate dibasic and sodium tripolyphosphate induced precipitation when alternated with 100mM $CaCl_2$ incubations.

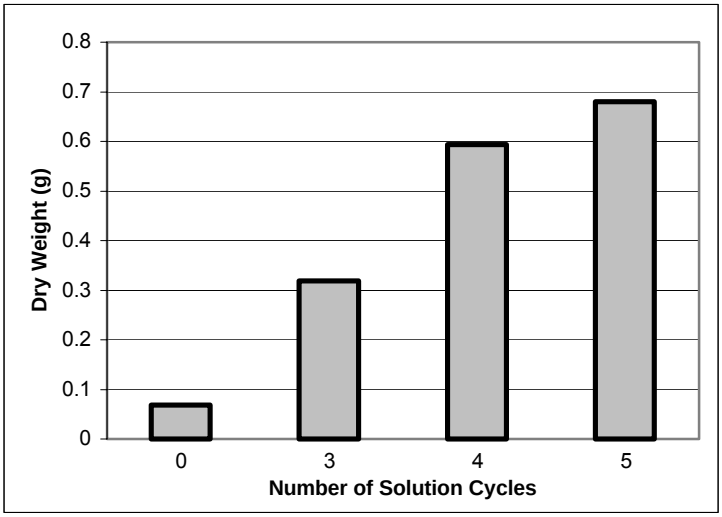

Figure 3.4: Weight Increase of Dried Bacterial Cellulose with Varying Number of Incubation Cycles of 100mM $CaCl_2$ and 60mM Na_2HPO_4

Weight is for a single pellicle after incubation in salt solution

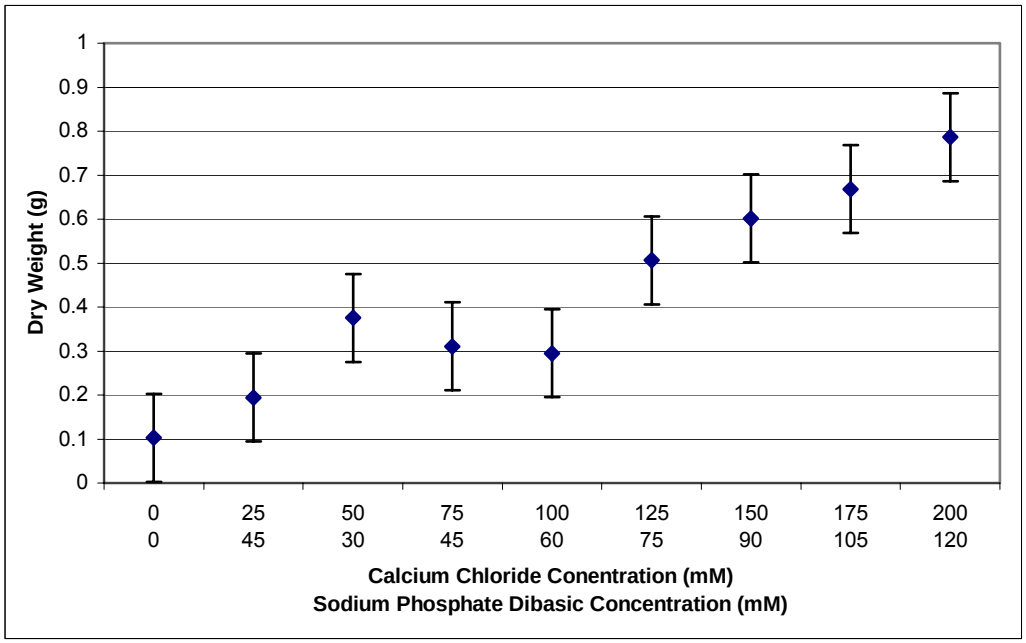

Figure 3.5: Weight Increase of Dried Calcium-Phosphate Bacterial Cellulose with Varied Molarities of Calcium and Phosphate Incubation Solutions

Weight is for a single pellicle after incubation in salt solution

At this time, the exact mechanism of the calcium phosphate deposition is not known. It is hypothesized that the precipitation of apatite is enabled either by the chemical structure of the bacterial cellulose, the physical structure of the cellulose, or a combination of both.

It has been hypothesized in several papers that highly polar function groups, such as hydroxyl, carboxyl, and phosphate groups; trigger the precipitation of apatite (84). Techniques have been specially developed to induce the formation of hydroxyl groups on materials which then enabled the nucleation of apatite on the material surface (11).

Cellulose has an abundance of hydroxyl groups. It is possible that a negative dipole moment produced by the oxygen in neighboring hydroxyl groups may form a weak bond with the calcium cation. Because the bond is weak, it enables the calcium cation to further bond with phosphate anions (Figure 3.6). In this way, the minerals may be formed along the cellulose fibrils. As the cellulose is repeatedly incubated in salt solutions, more ions are available to saturate the hydroxyl groups, and more calcium phosphate mineral can form.

This is similar to the structure of alginate in the presence of cations as discussed in an article by Dumitriu et al. (41). Chelation places Ca^{2+} ions in between the poly-L-guluronate chain sequences of the alginate. C-NMR spectra of alginate with various Ca^{2+} concentrations indicate

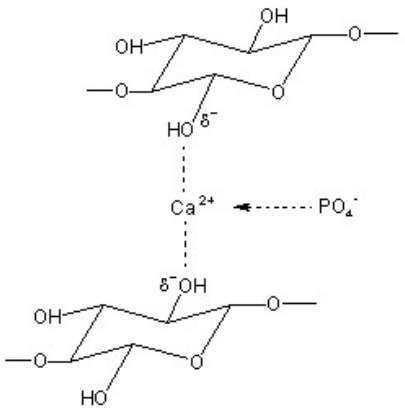

Figure 3.6: Proposed Mechanism of Apatite Induction

Image created on ChemDraw®

that the carboxyl, hydroxyl, and possibly the ring oxygen atoms in the guluronate residues are involved in binding to the Ca^{2+} ions. These bonds cause the guluronate chain segments to buckle into an "egg-box" model (41) (Figure 3.7). Due the extensive presence of hydroxyl and ring-oxygen atoms in cellulose, a similar mechanism may be occurring in the calcification of bacterial cellulose.

An alternate theory is that the unique structure of the cellulose permits the deposition of the calcium phosphate. Though the cellulose is highly porous and allows ions to freely enter into the matrix, the size of the pores is relatively small. Bacterial cellulose is composed of densely packed microfibrils with minute hollow spaces. Scanning electron microscopy (Microspec WDX) was performed on freeze-dried cellulose produced by the *Gluconacetobacter hansenii* strain coated with gold (Hummer VI Sputtering System, Technics). The tunnels between the fibrils are estimated to be approximately 100–300 nm in diameter (Figure 3.8 following page). This constrains the loading of solutes within the cellulose preventing large particles to form. The net result is a fine homogeneous precipitation within the cellulose matrix. Because they are securely

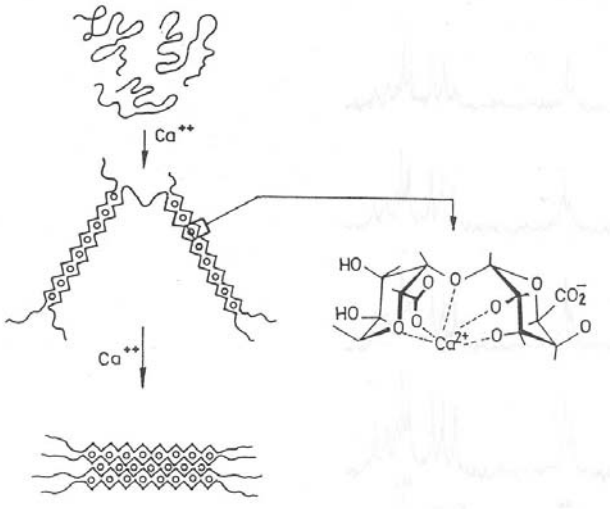

Figure 3.7: Egg-box Model of Calcium Interaction with Alginate Gel Network

Ca^{2+} are represented by circles occupying interstices in lateral associations of buckled guluronate chain segments (41)

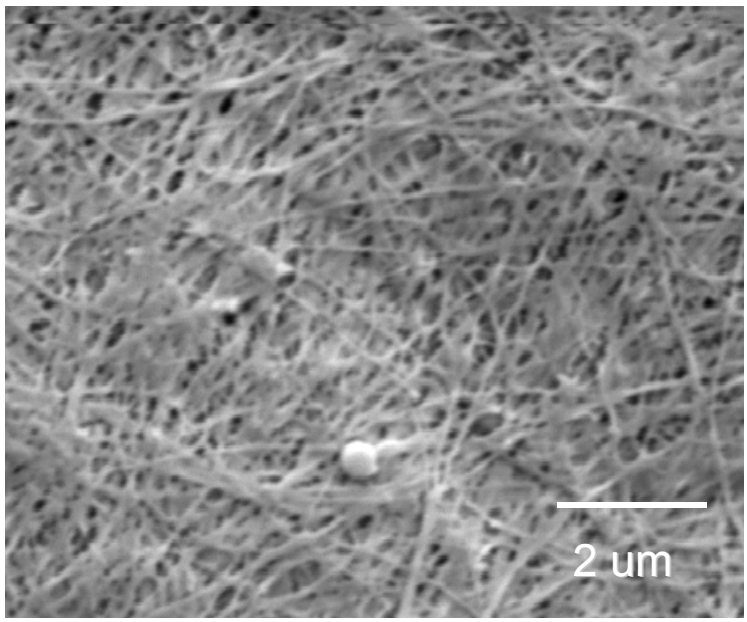

Figure 3.8 SEM Image of Freeze-Dried Bacterial Cellulose

Micrograph taken at Oak Ridge National Laboratory

positioned within the fibrils, the particles formed cannot leave the matrix.

3.2.2 Incubation in Simulated Body Fluid

After native bacterial cellulose was soaked in SBF, visible white precipitate formed in the matrix (Figure 3.9, following page). A 4±1 fold increase in thickness and a 1.3 ± 0.1 fold increase in weight was observed. When cellulose that had already been precipitated with calcium chloride and sodium phosphate dibasic was incubated in simulated body fluid, it increased 1.26 ± 0.08 fold in weight and 1.31 ± 0.05 fold in thickness. Again, the increase in weight and thickness was attributed to the apatite formed in the cellulose.

As was mentioned before, Kokubo et al. have performed numerous studies inducing apatite formation with simulated body fluid (10, 11). Simulated body fluid experiments were carried out with bacterial cellulose to see if apatite formation would occur. Kokubo et al. stated that functional groups nucleate apatite when in contact with the fluid which grow by consuming the calcium and phosphate ions in the surrounding body fluid (10,11). Hydroxyl groups are

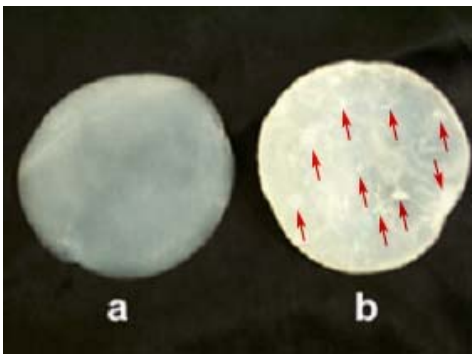

Figure 3.9: Precipitation of Apatite in Bacterial Cellulose by Incubation in Simulated Body Fluid

Left: Dried unaltered bacterial cellulose
Right: Dried bacterial cellulose after incubation in simulated body fluid. Red arrows indicate areas of white precipitate.

among these functional groups. This may account for the apatite formation in the cellulose after incubation in simulated body fluid. As was discussed in the previous section, the hydroxyl groups may be forming a weak bond with calcium ions. The calcium ions may then be attracting the phosphate ions forming atomic clusters at the hydroxyl groups. It is believed the atomic clusters form a calcium phosphate precursor of the form $Ca_3(PO_4)_2$. The $Ca_3(PO_4)_2$ units eventually transition to hydroxyapatite (11).

Several formulations of simulated body fluid were researched before selecting one to use in this investigation. Hank's Solution (85) and protocols developed by Kokubo (11) and Tas (12) were evaluated. When these compositions of these fluids are compared to the actual salt concentration of plasma, it appears the protocol developed by Tas most closely resembles blood plasma (Table 3.1, following page). Consequently, the simulated body fluid protocol by Tas was used in this investigation.

Table 3.1: Three Methods for Preparing Simulated Body Fluid

Ion	Blood Plasma	Hank's Solution (85)	Kokubo (11)	Tas (12)
Na^+	142.0 mM	160.0 mM	142.0 mM	142.0 mM
Cl^-	103.0 mM	143.0 mM	148.8 mM	125 mM
HCO_3^-	27.0 mM	4.2 mM	4.2 mM	27.0 mM
K^+	5.0 mM	11.2 mM	5.0 mM	5.0 mM
Mg^{2+}	1.5 mM	1.0 mM	1.5 mM	1.5 mM
Ca^{2+}	2.5 mM	1.3 mM	2.5 mM	2.5 mM
HPO_4^{2-}	1.0 mM	1.0 mM	1.0 mM	1.0 mM
SO_4^{2-}	0.5 mM	0.2 mM	0.5 mM	0.5 mM

3.2.3 Phosphorylated Cellulose in Calcium Solutions

3.2.3.a Characterization of Phosphorylated Cellulose

As mentioned previously in section 1.3.4.d, phosphorylation attaches phosphate groups to the cellulose. In the present study, the extent of phosphorylation was quantified by measuring the ion exchange capacity of the modified cellulose. A potentiometric titration of the phosphate groups was carried out. An example of such a titration was performed on the acidified cellulose with sodium hydroxide. The pH of the solution is graphed against the amount of NaOH added to the solution (Figure 3.10, following page). It can be inferred from the graph that the equivalence point was reached after the addition of 205 µmol NaOH. This indicates that 205 µmol of phosphate groups were present in the 0.161 g of cellulose, or 1.273 µmol/g.

3.2.3.b Apatite Deposition on Phosphorylated Cellulose

After the phosphorylated cellulose was incubated in the various calcium salts, a white precipitate was found to be deposited throughout the matrix. The phosphorylated samples increased in weight after incubation, indicating salt deposition (Figure 3.11, following page).

However, the deposition was not as thick or as homogenous as with native cellulose incubated in $CaCl_2$ and Na_2HPO_4. Again, these weight increases were not as great as with the previous method using calcium chloride and sodium phosphate dibasic.

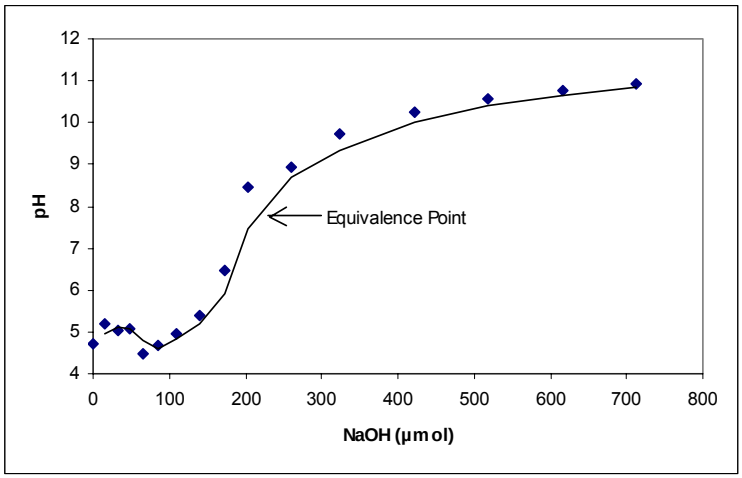

Figure 3.10: Titration of Acid-Treated Phosphorylated Cellulose with NaOH

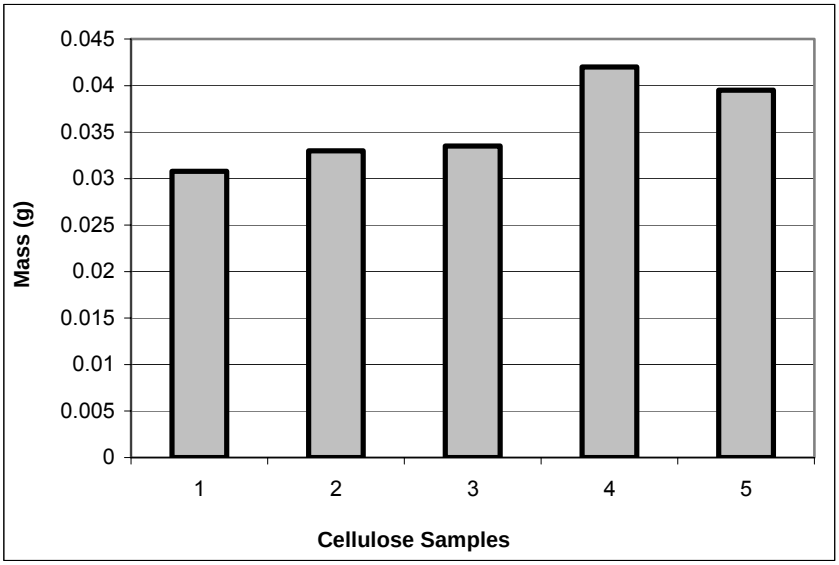

Figure 3.11: Measure of Apatite via Weight of Phosphorylated Bacterial Cellulose Incubated in Various Salt Solutions

1: Unaltered bacterial cellulose (one pellicle)
2: Phosphorylated BC incubated in 100mM $CaCl_2$ (one pellicle)
3: Phosphorylated BC incubated in 100mM $CaCl_2$ and in SBF (one pellicle)
4: Phosphorylated BC incubated in 12mM $Ca(OH)_2$ (one pellicle)
5: Phosphorylated BC incubated in 12mM $Ca(OH)_2$ and SBF (one pellicle)

Because the cellulose contains phosphate groups, they bind with calcium ions to form apatite. The calcium ions found in the calcium chloride, calcium hydroxide, and simulated body fluid combined with the phosphate groups and mineralized the bacterial cellulose. The thickest deposition and highest increase in weight occurred when the phosphorylated cellulose was incubated in aqueous calcium hydroxide. This may be because more calcium ions are present in this solution. It also may be because the OH^- ions present in the solution enhanced the binding of the calcium ions to the phosphate groups.

3.2.4 Incubation in Fluoride and Carbonate Solutions

After incubating the cellulose in calcium chloride and potassium fluoride, a thick white precipitate formed throughout the matrix. The dry weight of the cellulose increased 6 fold with a white precipitate while the thickness increased 12 fold.

After incubating the cellulose in calcium chloride and sodium carbonate, a thick white precipitate had also formed in the matrix. The dry weight of the cellulose increased 5 fold and the thickness increased 12 fold. The amount of precipitate and thickness of these depositions were comparable to that produced by calcium chloride and sodium phosphate dibasic.

The incorporation of carbonate and fluoride ions into the apatite was attempted because they are natural trace elements found in biological hydroxyapatite. The inclusion of these ions may produce an apatite more similar to that found in natural bone. This may induce a better tissue response.

Having carbonate or fluoride ions substituted in apatite also affects its dissolution rate. Incorporation of carbonate ions has been shown to increase apatite dissolution and may increase the bone replacement process after implantation (86). Apatites that contain fluoride ions are more likely to retard demineralization and dissolution (87). If used in dental applications, the presence of fluoride has been proven to resist caries (87).

3.3 Alizarin Red S Staining

Sodium 1,2-dihydroxyanthraquinone-3-sulfonate (Alizarin Red S) is a commonly used organic dye used in the histologic identification of calcium deposits. The two hydroxyl groups in Alizarin Red S enables a chelate formation with metal ions (Figure 3.12). It combines with calcium ions to form a red stain (88).

Calcium induction into the cellulose matrix was confirmed by staining with Alizarin Red S dye. One pellicle that had been incubated with $CaCl_2$ and Na_2PO_4, one pellicle that had been incubated with $CaCl_2$ and Na_2PO_4 followed by incubation in simulated body fluid, and one untreated cellulose pellicle were treated with Alizarin Red S. The mineralized samples became uniformly red throughout the sample (Figure 3.13, following page). Bacterial cellulose incubated in simulated body fluid was also stained with Alizarin Red S (Figure 3.14, following page).

The results from the Alizarin Red S staining indicated the distribution of calcium containing minerals in the cellulose. A homogeneous deposition of calcium apatite was observed with the cellulose incubated in $CaCl_2$ and Na_2HPO_4, and also when incubated in $CaCl_2$ and Na_2HPO_4 followed by incubation in simulated body fluid. This method of mineralization enables a uniform precipitation throughout the cellulose matrix. Cellulose incubated in only simulated body fluid did not produce a homogenous coating. Though the dye did confirm that calcium containing minerals formed, it is evident that the mineral did not coat as uniformly as the previous sample. Isolated apatite crystals are observed in Figure 3.14 as opposed to the homogeneous coating in

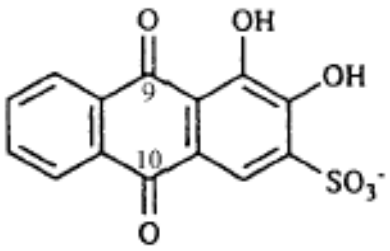

Figure 3.12: Compound Structure of Alizarin Red S (88)

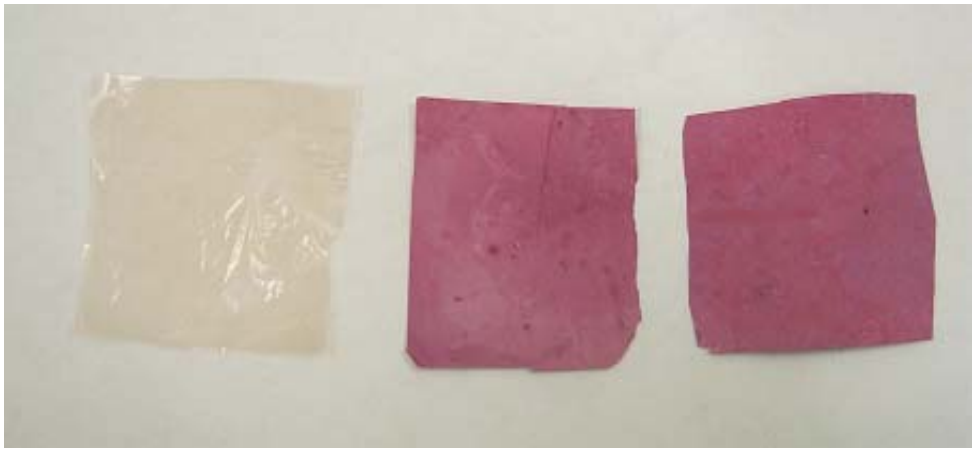

Figure 3.13: Calcium Phosphate Bacterial Cellulose Stained with Alizarin Red S

Left: Dried native bacterial cellulose stained with Alizarin Red S
Center: Dried calcium phosphate bacterial cellulose stained with Alizarin Red S
Right: Dried calcium phosphate bacterial cellulose after incubation in simulated body fluid stained with Alizarin Red S

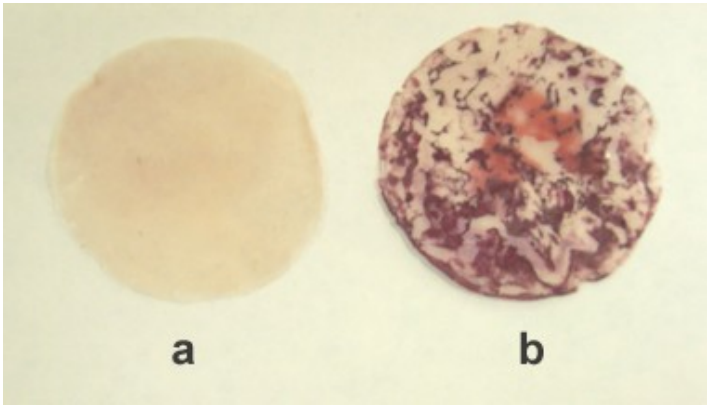

Figure 3.14: Alizarin Red S Staining on Bacterial Cellulose Incubated in Simulated Body Fluid

Left: Dried native bacterial cellulose stained with Alizarin Red S
Right: Dried bacterial cellulose after incubation in simulated body fluid stained with Alizarin Red S

Figure 3.13.

Thus, bacterial cellulose becomes more thoroughly mineralized when incubated in $CaCl_2$ and Na_2HPO_4 in comparison to cellulose incubated in simulated body fluid.

3.4 Determination of Calcium and Phosphorus Induction Using LIBS

Verification that calcium and phosphorus were into present in the bacterial cellulose matrix was obtained by using Laser Induced Breakdown Spectroscopy (LIBS). In LIBS, a laser transforms the material into a plasma spark. The spectral emissions from this spark can be evaluated by a spectrometer to determine the material's elemental breakdown. The peak wavelengths were identified as elemental components by using the NIST Standard Reference Database #38 (NIST Spectroscopic Database of Atomic and Atomic Ions). The peak at 422.8 nm indicates the presence of calcium. The peaks at 949 nm and 952.8 nm verify the presence of phosphorus (Figure 3.15, following page).

Because calcium and phosphorus were proven to exist in the incubated cellulose, it was assumed that these elements were responsible for the physical and chemical change in the matrix. It is hypothesized that calcium and phosphate were combining to form apatite in the cellulose. This mineralization could be attributed to the appearance and increase in weight and thickness of the treated cellulose.

3.5 X-Ray Diffraction

X-ray diffraction can be used to identify a substance based on its crystal structure. Crystals have a distinct arrangement of atoms with specific distances between them. When an x-ray beam is directed through a crystal, the different interatomic distances produce a series of reflections to form a diffraction pattern. The position and intensity of the diffraction peaks are indicative of the unique crystal structure. Hundreds of thousands of diffraction patterns have been collected in the Powder Diffraction File (PDF) (International Centre for Diffraction Data File: Newtown Square, PA). By using indexes like the Hanawalt Index, or database software such as Jade 6.0 (Materials Data Incorporated: Livermore, CA), it is possible to identify a material based on its x-ray diffraction pattern.

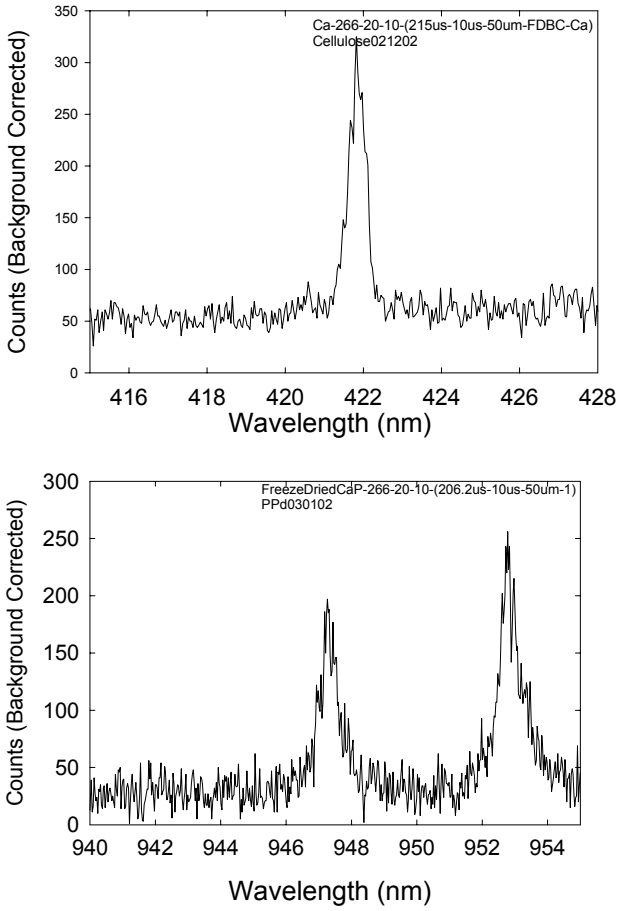

Figure 3.15: Laser Induced Breakdown Spectra of Freeze-Dried Native and Calcium Phosphate Bacterial Cellulose

Above: The peak at 422.8 nm indicates the presence of calcium.
Below: The peaks at 947.5 nm and 952.8 nm verify the presence of phosphorus.

Dried native bacterial cellulose (single pellicle) was first analyzed with x-ray diffraction (Figure 3.16, following page). The spectra had a distinct peak at 22.7° 2θ which corresponds to crystalline cellulose (89). X-ray diffraction was then performed on a pellicle of cellulose after it was incubated in calcium chloride and sodium phosphate dibasic and subsequently dried (Figure 3.17, following page). The diffraction pattern also had the peak at 22.7° 2θ indicating the presence of cellulose. The remaining peaks represented the diffraction pattern of the deposited mineral crystal. This unique array of peaks are characteristic of calcium deficient hydroxyapatite: $Ca_9HPO_4(PO_4)_5OH$ (CdHAP) (90). This pattern was matched using Jade 6.0, an x-ray diffraction processing software (Materials Data Incorporated: Livermore, CA).

The formation of calcium-deficient hydroxyapatite using this technique of deposition correlates with a study by Klein et al. (91). In that investigation, it was determined that only three thermodynamically stable calcium phosphates exist in aqueous solution. The identity of calcium phosphate depends on the solution pH. Monocalcium phosphate monohydrate ($Ca(H_2PO_4)_2 \cdot H_2O$) forms at pH < 2.5. Brushite ($CaHPO_4$) develops at a pH between 1.5 and 4.2. At a pH greater than 4.2, hydroxyapatite ($Ca_{10}(PO_4)_6(OH)_2$) is the most stable form (91). Because the pH of the incubation solutions in this procedure was greater than 4.2 (calcium chloride at pH 4.83 and sodium phosphate dibasic at pH 8.36), it was hypothesized prior to the x-ray diffraction results that this calcium phosphate was hydroxyapatite. The diffraction pattern confirmed that it was a form of hydroxyapatite. The presence of the cellulose peak amid the CdHAP peaks verifies that the material is a composite consisting of the ceramic particles within the cellulose substrate.

A Scintag XDS2000 Room Temperature X-Ray Diffractometer was used to identify cellulose deposited with mineral salts by other methods (Table 3.2, page 56). Only one of these patterns were able to give conclusive evidence: native cellulose incubated in calcium chloride and sodium carbonate. The x-ray diffraction pattern of the cellulose after it was incubated in calcium chloride and sodium carbonate is given in Figure 3.18 (page 56). Like the other diffraction pattern, the presence of the peak at 22.7° 2θ indicates the presence of cellulose. Another peak is located at 28° 2θ, however this phase was not identified. The remaining peaks are

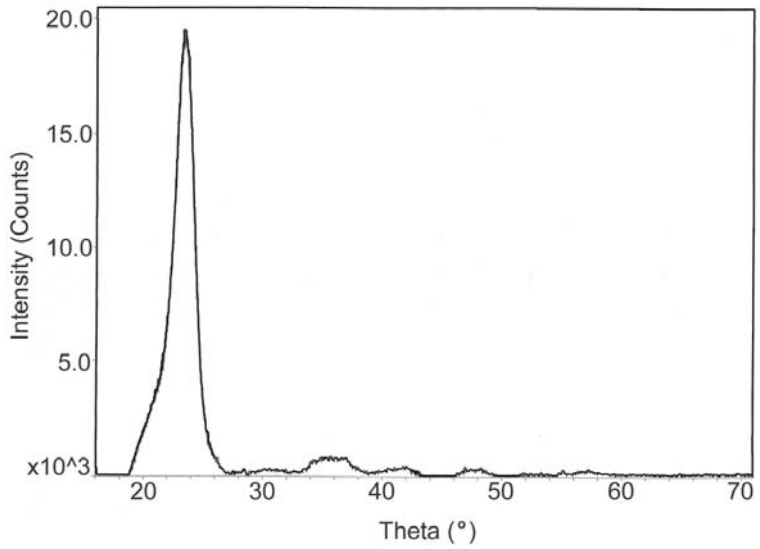

Figure 3.16: X-ray Diffraction Pattern of Dried Native Bacterial Cellulose

Peak at 22.7° theta corresponds to crystalline cellulose (89)

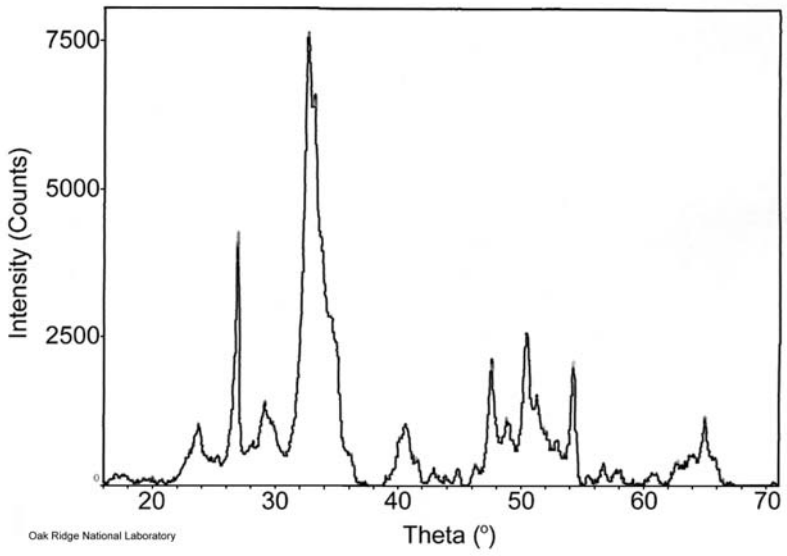

Figure 3.17: X-ray Diffraction Pattern of Dried Calcium Phosphate Bacterial Cellulose

Peak at 22.7° theta corresponds to crystalline cellulose, remaining peaks are characteristic of calcium deficient hydroxyapatite (90)

Table 3.2: Cellulose Samples Analyzed with the Scintag XDS2000 X-Ray Diffractometer

Type of Cellulose	Salt Solution used for Incubation
Native Bacterial Cellulose	Simulated Body Fluid
	100mM $CaCl_2$ and Simulated Body Fluid
	100mM $CaCl_2$ and 200mM KF
	100mM $CaCl_2$ and 100mM Na_2CO_3
Phosphorylated Bacterial Cellulose	Simulated Body Fluid
	100mM $CaCl_2$
	100mM $CaCl_2$ and Simulated Body Fluid
	12mM $Ca(OH)_2$
	12mM $Ca(OH)_2$ and Simulated Body Fluid

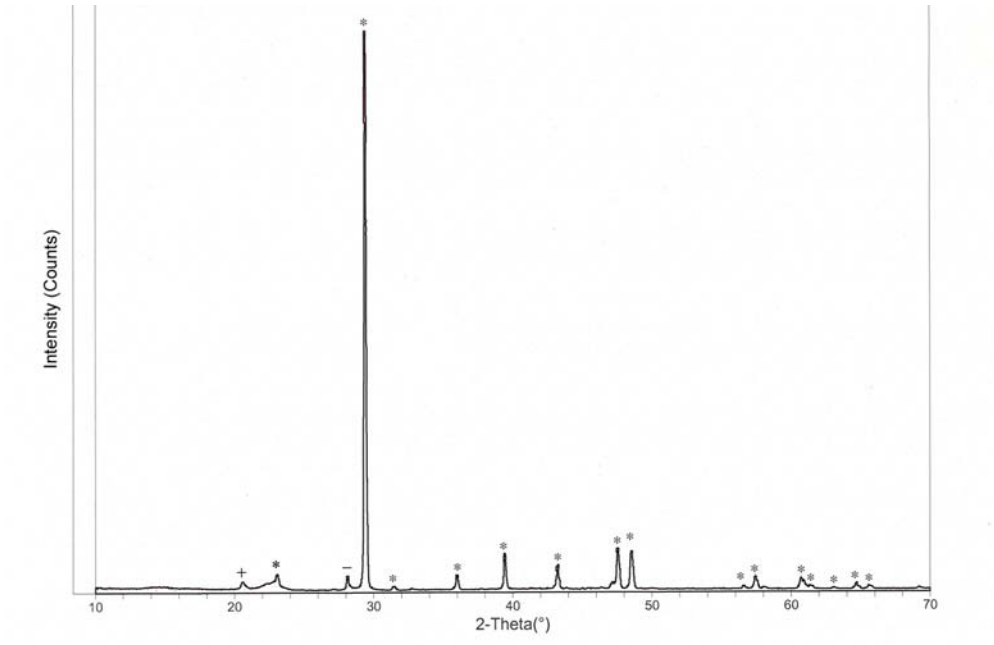

Figure 3.18: X-ray Diffraction Pattern of Dried Calcium Carbonate Bacterial Cellulose

Peaks represented by (*) are characteristic of calcium carbonate, (+) peak represents crystalline cellulose, peak represented by (-) is of unknown origin

characteristic of the mineral calcium carbonate. This pattern was also identified using Jade 6.0. The presence of the cellulose peak amid the calcium carbonate peaks verifies that the material is a composite consisting of the calcium carbonate and bacterial cellulose.

The diffraction pattern of NaCl contains a characteristic peak at 28° 2θ (92). It is possible that chloride ions from the $CaCl_2$ solution and sodium ions from the Na_2CO_3 solution may have combined to form NaCl salt. The existence of NaCl in the mineral matrix explains the presence of the peak at 28° 2θ in the diffraction pattern of Figure 3.18.

Diffraction patterns could not be obtained for the remaining eight samples listed in Table 3.2. One reason could be that the samples were too thin. The x-ray beam transmitted through the cellulose samples without diffracting the mineral crystals. Another reason could be that not enough mineral crystals were present to obtain a pattern. By having a small number of crystals in the cellulose, there is a smaller chance that the beam will come in contact with the atoms in the crystal lattice.

New samples must be made to obtain quantitative diffraction patterns. This can be done by growing thicker cellulose which can be loaded with more mineral deposition. Incubating the cellulose in more cycles of salt solutions, or in salt solutions with greater molarity, will increase the amount of precipitation. By having more mineral crystals in the matrix, there is a better chance that they will come in contact with the x-ray beam to form a complete diffraction pattern.

3.6 Biomimetic Formation of Apatite

This method of synthesizing CdHAP more closely resembles the physiological formation of apatite. As was mentioned earlier, traditional methods of HAP production utilize harsh chemicals at extreme temperature and pressure conditions. In natural bone formation, fibroblasts first deposit collagen fibrils to form the basis of the bone matrix. The osteoblasts then cause calcium and phosphorus salts to precipitate from blood plasma. These ions then bond with the collagen strands to mineralize the bone tissue. Thus, mineralization of physiological bone requires the deposition of salt ions from aqueous solutions. The formation of CdHAP on bacterial

cellulose is similar to this process. With refinements, this biomimetic technique may produce a more biologically equivalent apatite material that is more similar to physiological bone.

3.8 Mammalian Cell Culture Testing

In-vitro testing with mammalian cells is an established method to determine whether a material will function appropriately in a physiological environment. It is a useful preliminary tool to evaluate cytocompatibility without the complexity and sacrifice of living subjects. For an ideal biomaterial, isolated animal cells will use the matrix as a scaffold for attachment, proliferation, and differentiation. Because hydroxyapatite can bond with bone and is already used in several orthopedic devices (2), osteoblasts were used for the in-vitro evaluation of the compatibility of the produced calcium-deficient hydroxyapatite-bacterial cellulose matrix. The adhesion of the bone cells to an implant indicates that a solid fusion between the material and the bone tissue is possible. Thus the material may be used as a therapeutic implant to regenerate bone and heal osseous damage (93).

3.8.1 In-Vitro Testing of Native Bacterial Cellulose Vs. Calcium Phosphate Bacterial Cellulose

Prior to seeding, the cell counts of each of the cell suspensions were recorded (Table 3.3). After being combined with the cellulose, the cells were observed on a light microscope (100X magnification). The two pellicles of native cellulose and the two pellicles of mineralized cellulose did not appear to elicit a toxic response on the osteoblasts. Dead cells were not

Table 3.3: Cell Counts of Cell Suspension Prior to Seeding for First In-Vitro Experiment

Sample	Cell Count per mL of suspension
Unaltered Bacterial Cellulose Pellicle (UABC I)	290×10^4
Culture Dish of Unaltered Bacterial Cellulose Pellicle (UABC I)	283×10^4
Calcium Phosphate Bacterial Cellulose Pellicle (CPBC I)	388×10^4
Culture Dish of Calcium Phosphate Bacterial Cellulose Pellicle (CPBC I)	100×10^4
Control	165×10^4

observed in the media after culture. After three days of culture, it was observed with a light microscope that the cells had attached to the unaltered bacterial cellulose samples. The cells continued to grow and proliferate until the end of the ten-day period. At that time, the pellicles were removed from their culture conditions for evaluation. The opacity of the calcium phosphate bacterial cellulose prevented the observation of the cells using light microscopy.

Each of the four cellulose samples produced (UABC I, UABC II, CPBC I, CPBC II) were treated with trypsin to detach the cells. However, it was observed via a light microscope (100X magnification) that the trypsin treatment was not detaching all of the cells from the unaltered samples. Many cells were still attached to the cellulose after being treated with trypsin. This same mechanism may also have occurred with the calcium phosphate bacterial cellulose, though it could not be confirmed by light microscopy. It is postulated that the cells were tightly lodged within the tiny cellulose pores preventing cell dislodgment. It is also possible that the cell proteins used to adhere the cells onto the cellulose had been incorporated deep within the cellulose matrix. Osteoblasts also produce collagen as part of the extracellular matrix. The extracellular matrix may have integrated into the cellulose which secured the cells onto the substrate.

Using a higher concentration of trypsin or longer incubation times may have enabled the enzyme to induce complete detachment. A potential problem with this course is that extended exposure to trypsin may cause cell damage (94).

The culture dishes in which the cellulose and cells were incubated were also treated with trypsin to determine the fraction of cells attaching to the dish instead of the cellulose. If more cells had attached to the cellulose, this would suggest the cellulose is a favorable cell substrate. The cells from UABC I, the dish of UABC I, CPBC I, and the dish of CPBC I were stained with Trypan Blue and counted on a hemacytometer. These cell counts are given in Table 3.4 (following page). The cell counts for the unaltered bacterial cellulose pellicle, the calcium phosphate bacterial cellulose pellicle, and the dish where the calcium phosphate bacterial cellulose pellicle was cultured are low compared to the control and the dish where the unaltered bacterial cellulose pellicle was cultured. The low counts of the pellicles could be attributed to the

Table 3.4: Cell Counts of Cells After Detachment for First In-Vitro Experiment

Sample	Cell Count per mL of suspension
Unaltered Bacterial Cellulose Pellicle (UABC I)	3×10^4
Culture Dish of Unaltered Bacterial Cellulose Pellicle (UABC I)	101×10^4
Calcium Phosphate Bacterial Cellulose Pellicle (CPBC I)	3×10^4
Culture Dish of Calcium Phosphate Bacterial Cellulose Pellicle (CPBC I)	6×10^4
Control	90×10^4

fact that the cells were not fully detached from the cellulose. When comparing the cell counts of the culture dishes, there is a larger cell count in the dish of unaltered bacterial cellulose compared to the cell count of the dish of calcium phosphate bacterial cellulose. This can be attributed to the fact that more cells were attached to the calcium phosphate cellulose opposed to the culture dish. The osteoblasts preferentially occupied the calcium phosphate cellulose. Conversely, the cells did not prefer to attach to the unaltered bacterial cellulose and instead occupied the culture dish. This confirms that the osteoblasts have more of an affinity for the calcium phosphate cellulose as opposed to the unaltered bacterial cellulose.

The cells from UABC II, the dish of UABC II, CPBC II, and the dish of CPBC II were lysed and assayed for alkaline phosphatase. The results of the scan are given in Table 3.5 (following page). The final absorbance read at 410nm gives a final approximate of p-nitrophenol liberated. A stock of p-nitrophenol of known concentration was not available to prepare a standard curve, thus a quantitative measurement of the liberated p-nitrophenol was not calculated. Like the cell counts, there is greater amount of ALP found in the cells in the calcium phosphate pellicle as opposed to the dish it where was cultured. Therefore, cells favored attachment to the calcium phosphate pellicle. This proves that the calcium phosphate pellicle performs capably as a cell substrate. Because there is no appreciable difference between the amounts of ALP in the

Table 3.5: Alkaline Phosphatase Assay

Sample	Absorbance at 410nm
Unaltered Bacterial Cellulose Pellicle (UABC II)	0.2328
Culture Dish of Unaltered Bacterial Cellulose Pellicle (UABC II)	0.2264
Calcium Phosphate Bacterial Cellulose Pellicle (CPBC II)	0.6814
Culture Dish of Calcium Phosphate Bacterial Cellulose Pellicle (CPBC II)	0.0369
Control	1.0844

unaltered bacterial cellulose versus the dish, one can conclude that the unaltered bacterial cellulose pellicle is a passive substrate without a significant affinity for bone cells.

The cell counts and ALP assay indicate that good cell colonization can occur on the calcium phosphate cellulose once implanted. The calcium phosphate treatment appears to produce a favorable substrate to which the cells preferentially attach. Initial cell colonization enables a union between the implant and the tissue interface. Prolonged colonization may eventually result in the creation of newly functional bone throughout the implanted matrix.

3.8.2 In-Vitro Testing of Bacterial Cellulose Grown in Rich Media Vs. Synthetic Media

Two pellicles grown on synthetic media and the three pellicles grown on rich media were seeded with osteoblast cells to evaluate biocompatibility. The cell counts of each of the cell suspensions were recorded before seeding them onto the cellulose substrates (Table 3.6, following page). As before, the cell-substrate interaction was observed on a light microscope (100x magnification). Attachment and proliferation of the cells onto the cellulose substrates were observed after two days of culture. The cells continued to grow and proliferate until the end of the seven-day testing period.

After staining with Crystal Violet, photomicrographs were taken of the cells attached to the cellulose (Figure 3.19 and Figure 3.20, page 63). As is evident by the figures, there was much more attachment and proliferation of osteoblasts on the cellulose derived from synthetic

Table 3.6: Cell Counts of Cell Suspension Prior to Seeding for Second In-Vitro Experiment

Sample	Cell Count per mL of suspension
Rich Media Bacterial Cellulose (RBC I)	104×10^4
Rich Media Bacterial Cellulose (RBC II)	262×10^4
Rich Media Bacterial Cellulose (RBC III)	223×10^4
Synthetic Media Bacterial Cellulose (SBC I)	246×10^4
Synthetic Media Bacterial Cellulose (SBC II)	284×10^4

media. The cells attached to the synthetic cellulose had formed projections due to the assembly of cytoskeletal actin filaments (93). The sheet-like projections are called lamellipodia and the needle-like projections are called filopodia. These projections enable cell motility. After formation and fixation of the lamellipodium, the cells use adhesive interactions to generate the traction and energy required for cell movement (95). Motility is essential for nearly all cell processes including cell and tissue development and remodeling. It is important in tissue engineering because it enables the cells to populate the scaffold and eventually produce bone within the matrix.

Synthetic media is composed of inorganic reagents. Rich Schramm-Hestrin media contains yeast extract and bactopeptone. These contain complex proteins which are difficult to remove from the cellulose during purification. Because the synthetic media lacks these components, it is purer. The increased purity may have increased the biocompatibility of the substrate, producing a more favorable matrix for the cells to attach and proliferate. When producing bacterial cellulose for medical applications, it seems likely that using synthetic media would be more favorable.

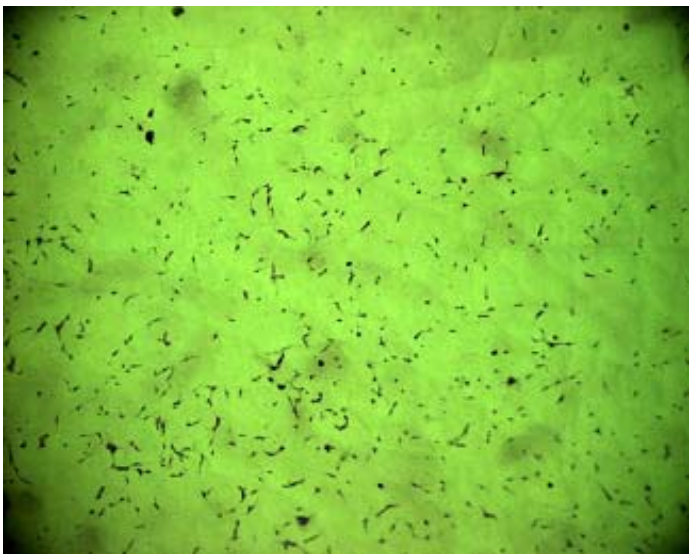

Figure 3.19: MC3T3-E1 Osteoblasts Grown for 7 days on Bacterial Cellulose Synthesized from Rich Media

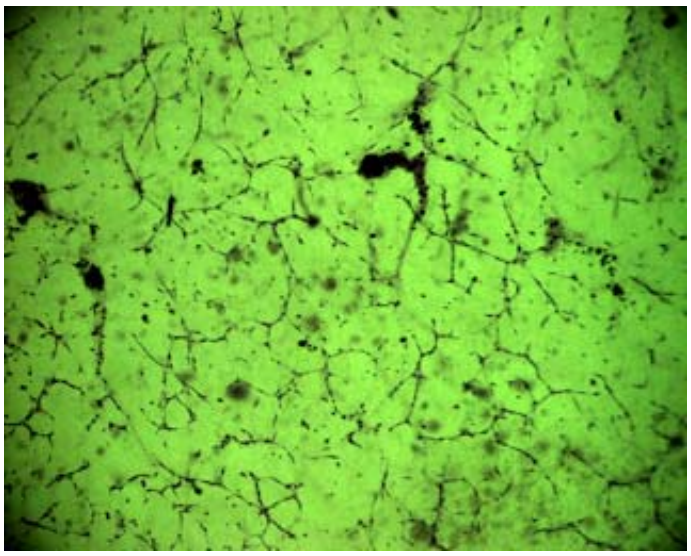

Figure 3.20: MC3T3-E1 Osteoblasts Grown for 7 days on Bacterial Cellulose Synthesized from Synthetic Media

Chapter 4

Conclusion and Future Work

4.1 Conclusion

In this study, several techniques were developed to deposit calcium phosphate particles into bacterial cellulose. Among these techniques were incubation of native cellulose in calcium chloride and sodium phosphate dibasic solutions, incubation of native cellulose in simulated body fluid, incubation of native cellulose in calcium chloride and sodium carbonate or potassium fluoride solutions, and incubation of phosphorylated cellulose in calcium solutions. Each of these techniques produced apatite which could be observed throughout the cellulose matrix.

Calcium induction in the cellulose was verified by staining with Alizarin Red S and Laser Breakdown Spectroscopy. The identity of two of the deposited minerals was confirmed using X-ray diffraction. Incubation in aqueous calcium chloride and aqueous sodium phosphate dibasic produced calcium-deficient hydroxypatite. Incubation in aqueous calcium chloride and aqueous sodium carbonate produced calcium carbonate.

Mammalian cell culture studies were conducted with osteoblasts to assess the biocompatibility of the substrates. Though cell attachment and proliferation was observed with native cellulose, especially with cellulose grown on synthetic media, proof of osteoblast attachment onto the calcium phosphate cellulose was not confirmed. However, it was proved that the composite was biocompatible and not cytotoxic.

The unique structure of bacterial cellulose enables the calcium phosphate particles to homogenously deposit into its matrix. This may be due to presence of many hydroxyl groups in cellulose which can form weak bonds with the calcium ions. The physical structure of the cellulose may also contribute to the homogenous deposition. The tiny pores within the cellulose enable the uniform loading of salt solutions. The pores also constrain the formation of the calcium phosphate salts to a small particulate size.

Many studies have verified the effectiveness of calcium deficient hydroxyapatite as a bioactive ceramic (13, 14, 17, 18). Bacterial cellulose has also been proven to be an effective

biomaterial (45, 65, 66). A composite of these two materials may be used as an orthopedic device.

4.2 Future Work

4.2.1 Additional X-Ray Diffraction

Additional x-ray diffraction (XRD) must be carried out to definitively identify the minerals deposited in the cellulose by the other techniques featured in this study. X-ray diffraction can also be used to measure particle size which is an important factor of biocompatibility with bone (6).

4.2.2 Additional Mammalian Cell Culture Testing

Further in-vitro testing must be carried out to ascertain whether the osteoblasts are truly attaching to the calcium-phosphate cellulose. This may be done by observing the surface with an environmental scanning electron microscope (ESEM). Traditional SEM methods require the samples to be evaluated under vacuum. This may damage biological samples. ESEM permits the imaging of hydrated biological samples by placing them in a low-vacuum chamber.

Methods to detach the cells from the cellulose must also be developed so that quantitative cell counts and alkaline phosphatase assays can be carried out. Some cell culturing manuals recommend thoroughly rinsing cells before detachment since serum present in the media contains trypsin inhibitors. Rinsing cells with EDTA before trypsinizing may also promote disaggregation. Higher concentrations of trypsin or EDTA may also enable thorough cell detachment (94).

4.2.3 Electron Microscopy

Scanning electron microscopy (SEM) provides three-dimensional quality surface images with excellent resolution and depth of field. It is hoped the future use of SEM can show where the particles are forming in the cellulose matrix, and how large the formed ceramic particles are. Observing the location of the different elements in the composite and viewing topography can be enhanced by using back-scattered electrons. Environmental scanning electron microscopy could be used to observe the hydrated CdHAP-BC composite.

Transmission electron microscopy has the ability to do electron diffraction and selected area diffraction. This enables phase identification which would be valuable in identifying the individual ceramic particulates in the cellulose matrix.

4.2.4 Fourier Transform Infrared Spectroscopy

Fourier Transform Infrared Spectroscopy (FTIR) can reveal information about a material's chemistry and structure orientation (96). It can identify the presence of functional groups and designate their location in the molecule. FTIR can be used to evaluate the bulk specimen, the surface, or used to perform depth profiling.

An FTIR spectrum may determine where the calcium phosphate molecules are adhering to the cellulose. It will show whether the calcium and phosphate ions are chemically bonding to the cellulose, or whether the apatite is simply precipitating on the surface or in the pores.

4.2.5 X-Ray Photoelectron Spectroscopy

X-Ray Photoelectron Spectroscopy (XPS) also gives information about individual elements in a material. Based on the spectra, it can be determined which compounds the elements are forming. Thus, the type of calcium phosphate present may be deducted based on XPS spectra.

Though XPS is does not provide quantitative results, semi-quantitative information can be obtained. The concentrations of the elements present in a sample can be determined relative to each other. For this application, the ratio of calcium composition versus phosphorus composition can be approximated using XPS. The Ca:P ratio and identification of calcium phosphate phases present are important data which can help gauge how a bioceramic will perform in-vivo.

Depth profiling can also be performed with XPS to see what phases are present on the surface.

4.2.6 Mechanical Testing

As important as chemical biocompatibility is in a biomaterial, mechanical compatibility is also imperative. Mechanical stresses and strains will inevitably be exerted onto the material once implanted. If the material fails under such conditions, it cannot be a successful tissue substitute.

Mechanical testing will provide information as to how the material will perform under load. Tensile and compressive tests under varying load rates will infer the material's strength, elasticity, ductility, creep, and viscous flow. Knowing how this material performs under various conditions will determine the applications for which it is appropriate (96).

References

(1) Hutchens SA, Woodward J, Evans BR, O'Neill HM: "Composite Material" (2002) U.S. Patent Application No. 10/295,461

(2) Hench LL. "Ceramics, Glasses, and Glass-Ceramics." In: *Biomaterials Science*. Ratner BD, Hoffman AS, Shoen FJ, Lemons JE (eds.) San Diego, CA: Academic Press, (1996). 73-84

(3) de Groot K. "Degradable Ceramics." In: *Biocompatibility of Clinical Implant Materials Volume I.* Williams DF (ed.) Liverpool, England: CC Press, (1981) 199-222

(4) Bensen CV, An YH, Friedman RJ. "Preclinical Evaluation of Bone Graft Substitutes." In: *Biomaterials and Bioengineering Handbook*. Wise DL (ed.) New York, NY: Marcel Dekker Inc. (2000) 699-714.

(5) Royer A, Viguie JC. "Stoichiometry of hydroxyapatite: influence on the flexural strength." *J. of Mat. Sci: Mat. In Med.* 4 (1993) 76-82

(6) Laquerriere P, Grandjean-Laquerriere A, Jallot E, Balossier G, Frayssinet P, Guenounou M. "Importance of hydroxyapatite particles characteristics on cytokines production by human monocytes in vitro." *Biomaterials* 24 (2003) 2739-2747

(7) Victora EC, Gnanam FD. "Synthesis and characterisation of biphasic calcium phosphate." *Trens Biomater. Artif. Organs* 16 (2002) 12-14

(8) Moore DC, Chapman MW, Manske D. "The evaluation of a biphasic calcium phosphate ceramic for use in grafting long-bone diaphyseal defects." *J. Orthop. Res.* 5 (1987) 356-365

(9) Gross K. "Hydroxyapatite – Synthesis of Hydroxyapatite Powders" http://www.azom.com/details.asp?ArticleID=1519

(10) Ohtsuki C, Kokubo T, Yamamuro T. "Mechanism of HA formation of CaO-SiO_2-P_2O_5. glasses in simulated body fluid." *J. Non-Cryst. Solids* 143 (1992) 84-92

(11) Kokubo T, Kim H-M, Kawashita M. "Novel bioactive materials with different mechanical properties." *Biomaterials* 24 (2003) 2161-2175

(12) Tas AC. "Synthesis of biomimetic Ca-hydroxyapatite powders at 37ºC in synthetic body fluids." *Biomaterials* 21 (2000) 1429-1438

(13) Vallet-Regi M, Rodriguez-Lorenzo LM, Salinas AJ, "Synthesis and characterization of calcium deficient apatite." *Solid State Ionics* 101-103 (1997) 1279-1285

(14) Mavrapoulos E, Rossi AM, da Rocha CC, Soares GA, Moreira JC, Moure GT. "Dissolution of calcium-deficient hydroxyapatite synthesized at different conditions." *Materials Characterization* 50 (2003) 203-207

(15) Narasarju TSB, Phebe DE. "Review: Some physico-chemical aspects of hydroxylapatite." *J. Mat. Sci.* 31 (1996) 1-21

(16) Han Y, Xu K, Lu J, Wu Z. "The structural characteristics and mechanical behaviors of nonstoichiometric apatite coatings sintered in air atmosphere." *J. Biomed. Mat. Res.* 45 (1999) 198-203

(17) Chern Lin JH, Kuo KH, Ding SJ, Ju CP. "Surface reaction of stoichiometric and calcium-deficient hydroxyapatite in simulated body fluid." *J. of Mat. Sci: Mat. in Med.* 12 (2001) 731-741

(18) Ducheyne P, Qiu Q. "Bioactive ceramics: the effect of surface reactivity on bone formation and bone cell function." *Biomaterials.* 20 (1999) 2287-2303

(19) Bourgeois B, Laboux O, Obadia L, Gauthier O, Betti E, Aguado E, Daculsi G, Bouler J-M. "Calcium-deficient apatite: a first in vivo study concerning bone ingrowth." *J. Biomedical Materials Research* 65A (2003) 402-408

(20) Alexander H. "Composites." In: *Biomaterials Science*. Ratner BD, Hoffman AS, Shoen FJ, Lemons JE (eds.) San Diego, CA: Academic Press, (1996). 94-105

(21) Ramakrishna S, Mayer J, Wintermantel E, Leong KW. "Biomedical applications of polymer-composite materials: a review." *Composites Science and Technology* 61 (2001) 1189-1224

(22) Alexander H. "Composites." In: *Biomaterials Science*. Ratner BD, Hoffman AS, Shoen FJ, Lemons JE (eds.) San Diego, CA: Academic Press, (1996). 94-105

(23) Visser SA, Hergenrother RW, Cooper SL. "Polymers." In: *Biomaterials Science*. Ratner BD, Hoffman AS, Shoen FJ, Lemons JE (eds.) San Diego, CA: Academic Press, (1996) 50-60

(24) Bonfield W, Behiri JC, Doyle C, Bowman J, Abram J. "Hydroxyapatite reinforced polyethylene composites for bone replacement." in *Biomaterials and Biomechanics,* Ducheyne P, Van der Perre G, Aubert AE, editors. (1984) 421-426

(25) Bakar MSA, Ceng MHW, Tang SM, Yu SC, Liao K, Tan CT, Khor KA, Cheang P. "Tensile properties, tension-tension fatigue and biological response of polyetheretherketone-hydroxyapatite composites for load-bearing orthopedic implants." *Biomaterials* 24 (2003) 2245-2250

(26) Bonfield W. "Composite Biomaterials." In *Bioceramics Vol. 9.* Kokubo T, Nakamoro T, Miyaji F. (eds.) Ois, Japan: Pergamon (1996) 11-13

(27) Wang X, Li Y, Wei J, de Groot K. "Development of biomimetic nano-hydroxyapatite/poly(hexamethylene adipamide) composites." *Biomaterials* 23 (2002) 4784-4791

(28) Wang M, Yue CY, Chua B. "Production and evaluation of hydroxyapatite reinforced polysulfone." *J. Mater. Sci. Mater. Med.* 9 (2001) 821-826

(29) Furuzono T, Sonoda K, Tanaka J. "A hydroxyapatite coating covalently linked onto a silicone implant material." *J. Biomed. Mat. Res.* 56 (2001) 9-16

(30) Durucan C, Brown PW. "Low temperature formation of calcium-deficient hydroxyapatite-PLA/PLGA composites." *J. Biomed. Mat. Res.* 51 (2000) 717-725

(31) Chang MC, Ko C-C, Douglas WH. "Preparation of hydroxyapatite-gelatin nanocomposite." *Biomaterials* 24 (2003) 2853-2862

(32) Kawashita M, Nakao M, Minoda M, Kim H-M, Beppu T, Miyamota T, Kokubo T, Nakamura T. "Apatite-forming ability of carboxyl group containing polymer gels in a simulated body fluid." *Biomaterials* 24 (2003) 2477-2484

(33) Varma HK, Yokogawa Y, Espinosa FF, Kawamoto Y, Nishizawa K, Nagata F, Kameyama T. Porous calcium phosphate coating over phosphorylated chitosan film by a biomimetic method." *Biomaterials* 20 (1999) 879-884

(34) Yin YJ, Zhao F, Song XF, Yao KD, Lu WW, Leong JC. "Preparation and characterization of hydroxyapatite/chitosan-gelatin Network Composite." *J. Appl. Polym. Sci.* 77 (2000) 2929-2000

(35) Ishikawa K, Kon M, Asaoka K, Miyamoto Y, Nagayama M. "Non-decay type fast-setting calcium phosphate cement: composite with sodium alginate." *Biomaterials* 16 (1995) 527-532

(36) Fricain JC, Granja PL, Barbosa MA, de Jeso B, Barthe N, Baquey C. "Cellulose phosphates as biomaterials. In vivo biocompatibility studies." *Biomaterials* 23 (2002) 971-980

(37) Oliveira AL, Malafaya PB, Reis RL. "Sodium silicate gel as a precursor for the in vitro nucleation and growth of a bone-line apatite coating in compact and porous polymeric structures." *Biomaterials* 24 (2003) 2575-2584

(38) Stephenson RL, Blackburn JB Jr. *The Industrial Wastewater Systems Handbook*. Lewis Publishers, NY (1998)

(39) Yannis, IV. "Natural Materials" In: *Biomaterials Science*. Ratner BD, Hoffman AS, Schoen FJ, Lemons JE (eds.) San Diego, CA: Academic Press, (1996) 84-94

(40) Walton AG, Blackwell J. *Biopolymers.* Academic Press (1973)

(41) Dumitru S, Vidal PF, Chronet E, "Hydrogels based on polysaccharides." In *Polysaccharides in Medicinal Applications.* Dumitru S (ed.) New York, Marcel Dekker (1996) 87-105)

(42) Miyamoto T, Takahashi S, Ito H, Inagaki H. "Tissue biocompatibility of cellulose and its derivatives." *Journal of Biomaterials Research* 23 (1989) 125-133

(43) Bielecki ES, Krystoynowicz, Turkiewicz M, Kalinowska H. "Bacterial Cellulose" *Biopolymers: Volume 5 Polysaccharides 1 and II*: (2001) 37-46

(44) Dictionary of Descriptive Terminology: http://palimpsest.stanford.edu/don/don.html

(45) Franz G, Baschek W. *Methods in Plant Biochemistry: Chapter 8 Cellulose.* (1990) 291-322

(46) Nishi Y, Uryu M, Yamanaka S, Watanabe K, Kitamura N, Iguchi M, Mitsuhashi S. "The structure and mechanical properties of sheets prepared form bacterial cellulose. Part 2: Improvement of the mechanical properties of sheets and their applicability of electroacoustic transducers." *J. of Mat. Sci.* 25 (1990) 2997-3001

(47) Stamboulis A. "Interface Modification for Natural Fibre Composites: A Review" Presentation at the 2nd International Conference on Eco-Composites (2001)

(48) Klemm D, Schumann D, Udhardt U, Marsch S. "Bacterial synthesized cellulose – artificial blood vessels for microsurgery." *Prog. Polym. Sci.* 26 (2001) 1561-1603

(49) Brown AJ. "On an Acetic Ferment which forms Cellulose." *J. Chem Soc.* 49 (1886) 432-439

(50) Schramm M, Hestrin S. "Factors affecting production of cellulose at the air- liquid interface of a culture of *Acetobacter xylinum*" *J. Gen. Microbiol.* 11 (1954) 123-129

(51) Budhiono A, Rosidi B, Taher H, Iguchi M. "Kinetic aspects of bacterial cellulose formation in nata-de-coco culture system." *Carbohydrate Polymers* 40 (1999) 137-144

(52) Iguchi M, Yamanaka S, Budhiono A. "Review: Bacterial cellulose-a masterpiece of nature's arts." *J. Materials Science* 35 (2000) 261-270

(53) White DG, Brown Jr. RM. "Prospects for the commercialization of the biosynthesis of microbial cellulose." In: *Cellulose and Wood – Chemistry and Technology.* Schuerch C (ed.) New York: Wiley, (1989) 573-90

(54) Yamanaka S, Watanabe K, Kitamura N. "The structure and mechanical properties of sheets prepared from bacterial cellulose." *J. of Materials Science.* 24 (1989) 3141-3145

(55) Cannon RE, Anderson SM, "Biogenesis of Bacterial Cellulose." *Crit. Reviews in Microbiol.* 17 (1991) 435-447

(56) Isihara M, Yamanaka S. "Modified bacterial cellulose." US Patent Application No. 20020065409 (2002)

(57) Bohn A, Fink H-P, Ganster J, Pinnow M. "X-ray texture investigations of bacterial cellulose." *Macromol. Cheml. Phys.* 201 (2000) 1913-1921

(58) Kim U-J, Kuga S, Wada M, Okano T, Kondo T. "Periodate Oxidation of Crystalline Cellulose." *Biomacromolecules* 1 (2000) 488-492

(59) Han T-Y, Chen C-C. "Crosslinking of Sulfonated Cotton Cellulose. Part I: Crosslinking and Physical Properties of DMDHEU-Treated Fabrics." *Textile Res. J.* 68 (1998) 115-120

(60) Tesoro GC, Willard JJ, "Crosslinked cellulose." In *Cellulose and Cellulose Derivatives, Vol 5.* Bikales NM, Segal L (eds.) New York, Wiley Interscience (1971) 835-875

(61) Hon DNS, "Cellulose and its Derivatives: Structures, Reactions, and Medical Uses." In *Polysaccharides in Medicinal Applications.* Dumitru S (ed.) New York, Marcel Dekker (1996) 87-105

(62) Saltzman WM. "Cell Interactions with Polymers." In *Principles of Tissue Engineering, 2nd Ed.* Lanza RP, Langer R, Vacanti J (eds.) San Diego CA, Academic Press (2000) 221-235

(63) Eiden-Assmann S, Viertelhaus M, Heiss A, Hoetzer KA, Felsche J. "The influence of amino acids on the biomineralization of hydroxyapatite in gelatin." *J. Inorg. Chem.* 91 (2002) 481-486

(64) Peppas NA. "Hydrogels" In: *Biomaterials Science*. Ratner BD, Hoffman AS, Schoen FJ, Lemons JE (eds.) San Diego, CA: Academic Press, (1996) 60-64

(65) Fontana JD, De Souza AM, Fontana CK, Torriani IL, Moreschi JC, Galliotti BJ, De Souza SJ, Narcisco GP, Bichara JA, Farah LFX. "Acetobacter cellulose pellicle as a temporary skin substitute." *Applied Biochemistry and Biotechnology.* 24/25 (1990) 253-264

(66) Novaes AB Jr., Novaes AB, Grisi FM, Soares UN, Gabarra F. "Gengiflex, an alkali-cellulose membrane for GTR: histologic observations." *Braz. Dent. J.* 4 (1991) 65-71

(67) Mello LR, Feltrin LT, Neto PTF, Ferraz FAP. "Duraplasty with biosynthetic cellulose: an experimental study." *Journal of Neurosurgery* 86 (1997) 143-150

(68) Watanabe K, Eto Y, Takano S, Nakamori S, Shibai H, Yamanaka S. “A new bacterial cellulose substrate for mammalian cell culture.” *Cytotechnology* 13 (1993) 107-114

(69) Eisele S, Ammon HPT, Kindervater R, Grobe A, Gopel W. “Optimized biosensor for whole measurements using a new cellulose based membrane.” *Biosensors and Bioelectronics* 9 (1994) 119-124

(70) Serafica G, Mormino R, Bungay H. “Inclusion of solid particles in bacterial cellulose.” *Appl. Microbiol. Biotechnol.* 58 (2002) 756-760

(71) Evans BR, O'Neill HM, Malyvanh VP, Lee I, Woodward J. "Palladium-bacterial cellulose membranes for fuel cells." *Biosensors and Bioelectronics* 18 (2003) 917-923

(72) Yokogawa Y, Toriyama M, Kawamoto Y, Nishizawa K, Nagata F, Kameyama T. "Calcium phosphate compound-cellulose fiber composite material prepared in soaking medium at 36.5-60ºC" *J. Mater. Res.* 13 (1998) 922-25

(73) Granja PL, Barbosa MA. "Cellulose phosphates as biomaterials. Mineralization of chemically modified regenerated cellulose hydrogels." *J. of Mat. Sci.* 36 (2001) 2163-2172

(74) Rhee S-H, Tanaka J. "Hydroxyapatite formation on cellulose cloth induced by citric acid." *J. Mat. Sci: Mat. in Med.* 11 (2000) 449-452

(75) American Academy of Orthopaedic Surgeons “Bone Graft Substitutes Safe, Effective.” *AAOS Bulletin*, Vol. 47 No. 5, October 1999

(76) Takaoka K, Yoshikawa H, Miyamoto S, Hashimoto J, Matsui Masahi, Ono K. “Bone-inducing factors in osteoinductive implants.” In *Human Biomaterials Applications*, DL Wise, DJ Trantolo, DE Altobelli, MJ Yaszemski, JD Gresser (eds.) New Jersey, Humana Press (1996) 91-98

(77) Burg KJL, Porter S, Kellam JF. "Biomaterial developments for bone tissue engineering." *Biomaterials* 21 (2000) 2347-2359

(78) Hutmacher DW. "Scaffolds in tissue engineering bone and cartilage." *Biomaterials* 21 (2000) 2529-2543

(79) Martson M, Viljanto J, Hurme T, Saukko P. “Biocompatibility of cellulose sponge with bone.” *Eur. Surg. Res.* 30 (1998) 426-432

(80) Nakabayashi N. "Dental biomaterials and the healing of dental tissue." *Biomaterials* 24 (2003) 2437-2439

(81) Head AJ, Kember NF, Miller RP, Wells RA. “Ion-exchange Properties of Cellulose Phosphate.” *J. Chem. Soc.* (1958) 3418-3425

(82) Lowry OH, Roberts NR, Wu M-L, Hixon WS, Crawford EJ. “The quantitative histochemistry of brain. II. Enzyme Measurements.” *J. Biol. Chem.* 105 (1954) 424-429

(83) Hakeda Y, Nakatani Y, Hiramatsu M, Kurihara N, Tsunoi M, Ikeda E, Kumegawa M. “Inductive effects of prostaglandins on alkaline phosphatase in osteoblastic cells, clone MC3T3-E1.” *J. Biochem.* 97 (1985) 97-104

(84) Tanahashi M, Yao T, Kokubo T, Minoda M, Miyamoto T, Nakamura T, Yamamuro. "Apatite coated on organic polymers by biomimetic process: Improvement in its adhesion to substrate by glow-discharge treatment" *J. Biomed. Mater. Res.* 29 (1995) 349-357

(85) Chern Lin JH, Kui KH, Ding SJ, Ju CP. *J. of Mat. Sci.: Mat. in Med.* 12 (2001) 731-741

(86) Miyamoto Y, Taketomo T, Ishikawa K, Yuasa T, Nagayama M, Suzuki K. "Effect of added $NaHCO_3$ on the basic properties of apatite cement." *Journal of Biomedical Materials Research* 54 (2001) 311-319

(87) Leamy P, Brown PW, TenHuisen K, Randall C. "Fluoride uptake by hydroxyapatite formed by the hydrolysis of α-tricalcium phosphate." *Journal of Biomedical Materials Research* 42 (1998) 458-464

(88) Wu L, Forsling W, Holmgren A. "Surface Complexation of Calcium Minerals in Aqueous Solution. 4. The Complexation of Alizarin Red S at Fluorite-Water Interfaces." *J. of Coll. and Interface Sci.* 224 (2000) 211-218

(89) Borysiak S, Garbarczyk J. "Applying the WAXS method the estimate the supermolecular structure of cellulose fibres after mercerisation." *Fibres and Textiles* 11 (2003) 104-106

(90) Mortier A, Lematire J, Rodrique L, Rouxhet PG, "Synthesis and Thermal Behavior of Well-Crystallized Calcium-Deficient Phosphate Apatite." *J. of Solid State Chem.* 78 (1989) 215-219

(91) Klein CPAT, de Blieck-Hogervorst JMA, Wolke JGC, de Groot K. "Studies of the solubility of different calcium particles in vitro." *Biomaterials* 11 (1990) 509-512

(92) *Selected Powder Diffraction Data for Education and Training: Search Manual and Data Cards.* JCPDS, International Centre for Diffraction Data: Swarthmore, PA (1988)

(93) Anselme K, "Osteoblast adhesion on biomaterials." *Biomaterials* 21 (2000) 667-681

(94) Mediatech Technical Library, Mediatech Incorporated: Herndon, VA. http://www.cellgro.com/tech/dload/tips/Trypsinizing_Monolayers.pdf

(95) Fletcher DA, Theriot JA. "An introduction to cell motility for the physical scientist." *Physical Biology* 1 (2004) 1-10

(96) Ratner BD. "Surface properties of materials." In: *Biomaterials Science*. Ratner BD, Hoffman AS, Schoen FJ, Lemons JE (eds.) San Diego, CA: Academic Press, (1996) 21-35

Appendix

Appendix A. List of Symbols and Abbreviations

Ca:P	Calcium to phosphorus ratio
BC	Bacterial Cellulose
HAP	Hydroxyapatite
sHAP	Stoichiometric Hydroxyapatite
CdHAP	Calcium-Deficient Hydroxyapatite
SBF	Simulated Body Fluid
ATCC	American Type Culture Collection
NaOH	Sodium Hydroxide
SDS	Sodium Dodecyl Sulfate
$CaCl_2$	Calcium Chloride
Na_2HPO_4	Sodium Phosphate Dibasic
KF	Potassium Fluoride
Na_2CO_3	Sodium Carbonate
XRD	X-Ray Diffraction
αMEM	Alpha Minimum Essential Medium Eagle
FBS	Fetal Bovine Serum
PBS	Phosphate Buffered Saline
ALP	Alkaline Phosphatase
ESEM	Environmental Scanning Electron Microscopy
SEM	Scanning Electron Microscopy
FTIR	Fourier Transform Infrared Spectroscopy
XPS	X-ray Photoelectron Spectroscopy

Vita

Stacy Hutchens was born in Vallejo, CA on February 9, 1979. She moved to Suffield, Connecticut at the age of 3; and then to Saratoga Springs, New York at the age of 4. She went to grammar school at Dorothy Nolan Elementary in Saratoga Springs NY, and then onto Saratoga Springs Junior High School. She graduated from Saratoga Springs Senior High School in June of 1997.

Stacy then went to The Cooper Union for the Advancement of Science and Art in New York City on a full tuition scholarship. There she received a Bachelor's of Science degree in Engineering with a focus in Biomedical Engineering.

After graduating from The Cooper Union in May 2001, Stacy moved to Knoxville Tennessee in January 2002. There she worked as a research assistant at Oak Ridge National Laboratory under the Oak Ridge Institute of Science and Engineering Higher Educational Experiences program. She works in the Chemical Sciences Division of Dr. Elias Greenbaum's Molecular Bioscience and Biotechnology Group under the tutelage Dr. Barbara Evans and Dr. Hugh O'Neill.

In August of 2002, she enrolled in The University of Tennessee's Graduate Program in the Department of Mechanical, Aerospace, and Biomedical Engineering. She was awarded the National Science Foundation Graduate Research Fellowship in the summer of 2003. Stacy received her Master of Science Degree in Engineering Science in May 2004. She is currently pursuing her Doctorate Degree in Biomedical Engineering at the University of Tennessee.